

ScholarWorks@GSU

Epidemiological Game-theory Dynamics of the co-evolution of Infodemic and Pandemic with Vaccination

Authors	Owoeye, Seyifunmi Michael
Citation	Owoeye, Seyifunmi Michael. "Epidemiological Game-theory Dynamics of the co-evolution of Infodemic and Pandemic with Vaccination." 2022. Thesis, Georgia State University. https://doi.org/10.57709/30436023
DOI	https://doi.org/10.57709/30436023
Download date	2026-06-06 20:43:24
Link to Item	https://hdl.handle.net/20.500.14694/10479

Epidemiological Game-theory Dynamics of the co-evolution of Infodemic and Pandemic
with Vaccination

by

Seyifunmi M Owoeye

Under the Direction of Yi Jiang, PhD

A Thesis Submitted in Partial Fulfillment of the Requirements for the Degree of

Master of Science

in the College of Arts and Sciences

Georgia State University

2022

ABSTRACT

COVID-19 pandemic, a highly infectious disease, has led to unprecedented health and socio-economic crisis worldwide. Accompanied by COVID-19 and its vaccination is an overabundance of misinformation promoting unhealthy practices among individuals. We propose a stratified SIS model incorporating an evolutionary game theoretical framework to help understand the simultaneous progression of pandemic and infodemic when vaccination is available. We consider two domains, disease and information domain, and assume that the information domain consists of the good and bad-behaving individuals. We assume that only the infected individuals with bad information can produce secondary cases of the infection. Findings indicate that the weight of good information does not significantly change the system's dynamics. Instead, it changes the system's stability with low risk requiring a higher weight of good information to arrive at a stable solution of lower infection and higher vaccination. Further, we found that we have an epidemic without misinformation management.

INDEX WORDS: COVID-19, Pandemic, Misinformation, Vaccination, Domain, Game Theoretical framework, Infodemic

Copyright by
Seyifunmi M Owoeye
2022

Epidemiological Game-Theory Dynamics of the Co-evolution of Infodemic and Pandemic
with Vaccination

by

Seyifunmi M Owoeye

Committee Chair: Yi Jiang

Committee: Gengsheng Qin

Gerardo Chowell

Yichuan Zhao

Electronic Version Approved:

Office of Graduate Services

College of Arts and Sciences

Georgia State University

August 2022

DEDICATION

This work is dedicated to the Most High God for the grace and strength bestowed upon me to complete this project work.

ACKNOWLEDGEMENTS

I express profound gratitude to God Almighty for His matchless grace and protection over my life and for keeping me in sound health and state of mind to see this work through to completion. May His name be exalted forever.

I will forever remain grateful to my advisor, Dr. Yi Jiang, under whose gentle supervision I successfully conducted this research. Her patience and shrewdness were elemental in my progress during this project. I also extend deep appreciation to the Graduate Coordinator, Dr. Gensheng Qin, and the entire staff of the department for their unwavering support and guidance.

This acknowledgment will not be complete if I do not mention my loving mother, Aderonke Owoeye, whose prayers and encouragement kept me going. I would also like to thank Adedamola Adebamiro for her unwavering support and for always edging me on. Lastly, I am grateful to all my friends for their care and love throughout my work. May the good Lord reward each one of you.

TABLE OF CONTENTS

ACKNOWLEDGEMENTS	VI
LIST OF TABLES	IX
LIST OF FIGURES	X
LIST OF ABBREVIATIONS	XIV
1	INTRODUCTION.....	1
1.1	Aim and Objectives of the Study	4
2	LITERATURE REVIEW	5
2.1	COVID-19 and Mathematical Modeling.....	5
2.1.1	<i>Susceptible-Infected-Recovered (SIR)</i>.....	5
2.1.2	<i>Susceptible-Exposed-Infected-Removed (SEIR)</i>.....	7
2.1.3	<i>Other Models</i>	10
2.2	Vaccination And Game Theory	12
3	MODEL FOR CO-EVOLUTION OF EPIDEMIC AND INFODEMIC.....	14
3.1	Game Theory and Vaccination: Deriving the Risk Function	18
3.2	Analytical Derivation of R_0 and Re	20
3.3	Calculation of the Jacobian Matrix.....	21
3.4	Obtaining the Nullclines	22
3.5	Perturbation About Fixed Points.....	24
4	RESULTS AND DISCUSSION	25
4.1	RICH DYNAMICAL PATTERNS OF THE MODEL	26

4.2	LOW-RISK PERCEPTION OF VACCINATION PROMOTES VACCINE UPTAKE	29
4.3	STOPPING MISINFORMATION IS NECESSARY TO STOP PANDEMIC	33
4.4	INCREASING EDUCATION REDUCES INFECTION AND PROMOTES VACCINATION.....	35
4.5	HIGH VACCINE EFFICACY INHIBITS DISEASE TRANSMISSION	37
4.6	INCREASING THE WEIGHT OF GOOD INFORMATION PROMOTES VACCINATION AND DECREASES INFECTION	40
5	CONCLUSION AND DISCUSSION	43
5.1	LIMITATIONS AND FUTURE DIRECTION	45
	REFERENCES.....	46

LIST OF TABLES

Table 3.1 Interpretation of the state variables and parameters. All parameters are unitless, except for γ measured in 1/day	18
Table 4.1 Model parameters, state variables, and their baseline values. $\hat{\chi}, \gamma, \chi$ and m are kept constant throughout the analysis.	25

LIST OF FIGURES

Figure 3.1 Schematic representation of the simultaneous progression of pandemic and infodemic with vaccination. Susceptible individuals with misinformation SB have an increased force of infection $\hat{\chi} > \chi$. Susceptible individuals with good information SG are infected with virus and misinformation at rates χ and μ respectively. Infected individuals with good information or bad information recover at the same rate γ . The misinformed infected IB become educated at rate ε . Additionally, a susceptible person with good information SG becomes vaccinated with probability ϕ . The leakage infection of the vaccinated population is asymptomatic and, therefore, unknowingly become IB15

Figure 4.1 Simple dynamical patterns emerged from the model. A - C: Disease-free equilibrium (stable node). (At misinformation $\mu = 7e - 07$). **D - F:** Simple periodic oscillations (stable limit cycle). At risk $r \in 0.127, 0.158$, misinformation $\mu \in (0.1, 0.144)$27

Figure 4.2 Simple dynamical pattern emerging from the model. A - C: Co-existence with high infection (stable focus). The other parameters are kept constant, as in Table 4.1. Initial conditions set about a perturbation of the steady states. **D - F:** Periodic large outbreaks at risk $r = 0.274$, misinformation $\mu = 0.1$. The other parameters are kept constant as in Table 4.1. Initial conditions set about a perturbation of the steady states.28

Figure 4.3 Complex dynamical pattern emerging from the model. A - C: Periodic large outbreaks at risk $r = 0.274$, misinformation $\mu = 0.1$. The other parameters are kept constant as in Table 4.1. Initial conditions set about a perturbation of the steady states.28

Figure 4.4: A – B Fixed Point with respect to risk r for Infected with bad information and vaccination, respectively. The dashed and solid lines represent unstable and stable branches, respectively. The system undergoes a branching point bifurcation (BP) at $r = 0.274$, a saddle node bifurcation (LP) at $r = 0.128$ and two Hopf bifurcation (H) at $r = 3.587$ and $r = 0.158$. **C – D:** Time evolution of a perturbation of the H bifurcation at $r = 3.587$ corresponding to a stable focus and the effective reproductive number Re31

Figure 4.5 A – B: Time evolution of a perturbation of the H bifurcation with a pair of purely imaginary eigenvalue at $r = 0.158$ corresponding to a stable limit cycle of low amplitude and the effective reproductive number Re . **C – D:** Time evolution of a perturbation of the BP bifurcation at $r = 0.274$ corresponding to a stable limit cycle and Re . **E – F:**Time evolution of a perturbation of the saddle-node bifurcation LP at $r = 0.127$ corresponding to a stable focus of high amplitude & Re32

Figure 4.6: A – B: Fixed Point with respect to misinformation μ for Infected with bad information and vaccination, respectively for $r = 3.587$ vs $r = 0.158$. The dashed and solid lines represent unstable and stable branches, respectively.....33

Figure 4.7: Fixed Point with respect to misinformation μ for Infected with bad information and vaccination, respectively for $r = 0.127$ vs $r = 0.158$. The dashed and solid lines represent unstable and stable branches, respectively. **C – D:** Time evolution of a perturbation of the saddle-node bifurcation LP at $\mu = 0.144$ corresponding to a stable focus of high vaccination and co-existence of infection & Re . **E – F:** Disease-free equilibrium (stable node). (At misinformation $\mu = 2.9e - 08$)34

Figure 4.8: A – B: Fixed Point with respect to education ϵ for Infected with bad information and vaccination, respectively for $r = 3.587$. The dashed and solid lines represent unstable and stable branches, respectively. **C – D:** Time evolution of a perturbation of

the LP bifurcation at $\epsilon = 0.063, r = 3.587$ corresponding to a steady state of zero vaccination and high infection & Re corresponding to a 100% bad-behaving population. **E – F:** Time evolution of a perturbation of the H bifurcation at $\epsilon = 0.450, r = 3.587$ corresponding to stable oscillation of low infection & Re36

Figure 4.9: A – B: Fixed Point with respect to education ϵ for Infected with bad information and vaccination, respectively for $r = 0.158$ vs 0.127 . The dashed and solid lines represent unstable and stable branches, respectively. **C – D:** Time evolution of a perturbation of the LP bifurcation at $\epsilon = 0.337, r = 0.158$ corresponding to a stable focus of high vaccination and co-existence of infection & Re37

Figure 4.10 A – B: Fixed Point with respect to vaccine efficacy, δ for Infected with bad information and vaccination, respectively for $r = 3.587$ vs $r = 0.158$. The dashed and solid lines represent unstable and stable branches, respectively.38

Figure 4.11: A – B: Time evolution of a perturbation of the H bifurcation at $r = 3.587, \epsilon = 0.450, 1, \delta = 0.714$ corresponding to stable oscillation of 8% infection and low vaccination & Re . **C – D:** Time evolution of a perturbation of the H bifurcation at $r = 3.587, \epsilon = 0.450, 1, \delta = 0.900$ corresponding to stable oscillation of low vaccination & Re39

Figure 4.12: A - D: Time evolution of a perturbation of the H bifurcation at $r = 0.158, \epsilon = 0.40, 1, \delta = 0.826$ drives the system to a stable focus of high vaccination and 18% infection corresponding to the co-existence of vaccination and infection & Re . **C – D:** Time evolution of a perturbation of the H bifurcation at $r = 0.158, \epsilon = 0.40, 1, \delta = 0.900$ corresponding to stable oscillation of low vaccination & Re40

Figure 4.13: Fixed Point with respect to the weight of education, α for Infected with bad information and vaccination, respectively for $r = 3.587$ (*green*) vs $r =$

0.158 (*red*). The dashed and solid lines represent unstable and stable branches, respectively. Increasing the weight of good information increases vaccination.41

Figure 4.14: **A:** Fixed Point with respect to the weight of education, α for Infected with bad information for $r = 3.587$ and the time evolution in the stable (solid lines) and unstable region (dashed lines). **B:** Time evolution of a perturbation of the H bifurcation at $r = 3.587, \mu = 0.1, \alpha = 1.0$ with low vaccination. **C :** Time evolution of a perturbation of the L bifurcation at $r = 0.158, \mu = 0.1, \alpha = 2.266$ drives the system to a stable focus of high vaccination and 18% infection corresponding to the co-existence of vaccination and infection. **D – E:** Fixed Point with respect to the weight of education, α for Infected with bad information for $\mu = 0.1$ *red* vs 0.144 *green* when $r = 0.158$ 42

LIST OF ABBREVIATIONS

BHRP: Bats-Hosts-Reservoir-People

BP: Branching Point Bifurcation

BT: Bogdanov-Takens

CDC: Centre for Disease Control.

CP: Cusp

DFE: Disease-Free Equilibrium

EVD: Ebola Virus Disease

H: Andronov Hopf Bifurcation

LP: Limit Point

MCMC: Markov Chain Monte Carlo

NPI: Non-pharmaceutical interventions

RP: Reservoir-People

SEAIR: Susceptible-Exposed-Asymptomatic-Infected-Recovered

SEIARW: Susceptible-Exposed-Symptomatic-Asymptomatic-Recovered-Seafood Market

SEIQR: Susceptible-Exposed-Infectious-Quarantined-Recovered

SEIR: Susceptible-Exposed-Infectious-Recovered

SIQR: Susceptible-Infectious-Quarantined-Recovered

SIR: Susceptible-Infected-Recovered

SIS: Susceptible-Infectious-Recovered

WHO: World Health Organization

1 INTRODUCTION

COVID-19 pandemic, a highly infectious disease caused by SARS - CoV -2 virus, has profoundly affected the world, leading to unprecedented health and socio-economic crisis. COVID-19 has infected about 525 million people worldwide, with approximately 6.3 million deaths reported as of May 24, 2022 (World Health Organization [WHO], 2022). To mitigate the spread of COVID-19, the world has adopted pharmaceutical (vaccines) and non-pharmaceutical interventions (NPIs). However, the non-pharmaceutical interventions (including frequent handwashing, social distancing, travel restriction, mask use, border shutdown, etc.) have become less effective over time (Nicola et al., 2020; Marzo et al., 2022). Thus, it is essential to develop effective vaccines as mass vaccination is the most potent way to manage COVID-19 transmission.

Although vaccines are the most reliable public health interventions in preventing the widespread transmission of an infectious disease such as SARS-CoV-2, their success depends on the uptake and the widespread belief about their benefit, as vaccine availability does not imply its acceptance among the world population (Hussein et al., 2015; Dror et al., 2020). This is proven by vaccine hesitancy, a strong reluctance or refusal to receive vaccination (MacDonald, 2015; Lazarus et al., 2020). The WHO has identified vaccine hesitancy as one of the top 10 global health threats in 2019 (World Health Organization [WHO], 2019). Vaccine hesitancy emanates from factors such as complacency, confidence issues, convenience/access, and risk perception (MacDonald, 2015; Betsch et al., 2018).

Research has found different factors to influence the COVID-19 vaccine hesitancy. The identified factors include concerns about the efficacy and safety of the vaccine (Neumann-Böhme et al., 2020; Rhodes et al., 2021; Soares et al., 2021; Liu et al., 2021; Solís Arce et al., 2021), distrust in scientists and healthcare personnel (Kreps and Kriner, 2020; Rozek et al.,

2021), socio-economic and demographic characteristics (e.g., education, marital status, occupation, etc.) (Soares et al., 2021; Vincent and Cordero, 2021), and conspiracy theories (Khan et al., 2020; Sallam et al., 2021).

In a speech made by WHO's director-general at the 2020 Munich Security Conference, he stated that "We are not just fighting a pandemic, we are fighting an infodemic" (World Health Organization [WHO], 2020b, February 15). An infodemic is the overabundance of good and bad information about infectious diseases and their mitigation approaches. COVID-19 and its vaccination have been accompanied by a vast amount of information (good and bad) and unconfirmed rumours from unfiltered outlets, often propagated via social media (Puri et al., 2020; Mills et al., 2020). It is challenging for the public to differentiate between facts, misinformation, opinions, or biases, resulting in the birth of uncertainty (Lancet Infectious Diseases Editorial Board, 2020). Misinformation regarding COVID-19 has promoted unhealthy practices that have helped propagate the spread of the disease, thereby posing a significant threat to public health (Tasnim et al., 2020).

Previous studies on infodemic have examined the distribution of infodemic on social media (Glowacki et al., 2016; Tran and Lee, 2016; Murayama et al., 2021). These studies suggest that misinformation was more widespread on social media than valuable information. A study used the susceptible-infectious-susceptible (SIS) model to examine the influence of media coverage on the spread of disease, incorporating the impact of media coverage in mitigating the spread of infection and showed that the spread of good information could decrease the basic reproductive number, thereby reducing the spread of the infection (Wang et al., 2013). Additionally, these models considered how the spread of information drives the spread of infection but lacked information about how the infection spread influences the spread of information.

With the world committed to combating COVID-19, there has been a wide range of research on COVID-19 infodemic. Most studies on COVID-19 infodemic are devoted to exploring its sources and how they contribute to the surge of bad information (Datta et al., 2020; Zhang et al., 2020; Naeem et al., 2021; Yang et al., 2021). The studies found a high incidence of good information and misinformation from social media platforms such as Twitter, Facebook, WhatsApp, YouTube, TikTok, etc. These studies are uniform in their conclusion, establishing the nexus between the spread of information and the spread of COVID-19. A study performed a comparative study of users' activity on five social media platforms, modelled the spread of information using epidemic models, and provided the basic reproductive number for each social media platform (Cinelli et al., 2020). A study used content analysis to identify the quantity, source, and characteristics of the COVID-19 infodemic and used topic modelling to group various themes of the infodemic (Zhang et al., 2021). Another study used an adjusted Susceptible-Exposed-Infectious-Recovered (SEIR) model for COVID-19 to explain how the use of social media influences disease spread. Their result suggested that social media promotes disease transmission by disseminating bad information. (Bae et al., 2021). Although these studies focused on how the spread of information is associated with the spread of infection, little has been done to provide information on the interaction between the spread of information, the spread of infection, vaccination and the perceived risk from infection and vaccination.

Our goal in this study is to propose a stratified SIS model that incorporates an evolutionary game theoretical framework to help understand the simultaneous progression of pandemic and infodemic when vaccination is available. We use an SIS model because it accounts for the possibility of reinfection by emerging new variants. The model considers two population groups; those influenced by good and bad information. The population with good information follows all CDC guidelines to mitigate the spread of COVID-19 and becomes vaccinated,

while those with bad information behave contrary and then promote the spread of the disease. Like the spread of infection, we assume that information spread requires a form of contact among the population, with people with good information getting misinformed by the bad and those with bad information getting re-educated by the good. In addition, we extend the work of Morciglio et al. (2021) by assuming that the probability of vaccination depends not only on the strength of the initiative parameter but also on the perception of risk of vaccination relative to infection and the weight of good information in risk calculation.

1.1 Aim and Objectives of the Study

This study aims to propose an SIS model to examine the co-evolution of pandemic and infodemic in the context of COVID-19, emphasizing evolutionary game theory. The objectives are to:

- 1.) Examine how infodemic in terms of misinformation influences disease transmission and drives vaccine uptake.
- 2.) Examine how education reduces infection and drives vaccination.
- 3.) Examine how risk perception of vaccination relative to infection promotes vaccination.
- 4.) Examine how vaccine efficacy influences the dynamics of a disease.
- 5.) Examine how the weight of good information in risk calculation drives vaccine uptake and infection.

2 LITERATURE REVIEW

2.1 COVID-19 and Mathematical Modeling

Recently, modelling and prediction of the SARS-COV-2 dynamics have become especially important in understanding the disease transmission and propagation, detecting the disease early and accurately, designing mass vaccination programs and examining current control strategies just to name a few (Khoshnaw et al., 2020; Mohamadou et al., 2020). Studies on the modelling of dynamics and transmission of COVID-19 have largely been based on the Susceptible-infected-recovered (SIR) model (Biswas et al., 2020; Chen et al., 2020; Chikina and Pegden, 2020; Gonzalez, 2020; Singh and Adhikari, 2020; Wang et al., 2020) and the Susceptible-Exposed-Infected-Removed (SEIR) model (Eikenberry et al., 2020; Guo et al., 2020; Pandey et al., 2020; Prem et al., 2020; Rădulescu et al., 2020; Zhan et al., 2020). Others have adopted Susceptible-Infectious-Quarantined-Recovered (SIQR) (Crokidakis et al., 2020), Susceptible-Exposed-Infectious-Quarantined-Recovered (SEIQR) (Vyasarayani and Chatterjee, 2020), Susceptible-Exposed-Symptomatic-Asymptomatic-Recovered-Seafood Market (SEIARW) (Zhao et al., 2020), Susceptible-Exposed-Asymptomatic-Infected-Recovered (SEAIR) (Shen et al., 2021), Markov Chain Monte Carlo (MCMC) (Wan et al., 2020).

2.1.1 Susceptible-Infected-Recovered (SIR)

Wang et al. (2020) proposed a Markov SIR model by incorporating several types of time-changing quarantine strategies including government-imposed mass isolation policies and micro-social distancing (self-quarantine and self-isolation) at the community level to develop a calibration procedure for under-reported infected cases. This model accounts for the time-changing probabilities of the susceptible, infected, recovered and dead compartments. The authors used the SIR model to examine the effect of current interventions on the COVID-19 pandemic within and outside Hubei in China by fitting the cumulative data into an empirical

form. They also reported that the model could be employed in predicting when daily proportions of removed cases would become more significant than the infected.

Singh and Adhikari et al. (2020) proposed an age-structured SIR model with social contact matrices and Bayesian imputation to study the development of the COVID-19 pandemic in India. The authors examined the influence of social distancing measures like workplace non-attendance, lockdown, and school closure on the transmission and propagation of the SARS-CoV-2. The authors showed that even with an equal probability of infection through contact, age, and social contact, differences in different populations result in a different basic reproductive number. They also reported that a three-week lockdown would be insufficient to mitigate the spread of the disease.

Chikina and Pegden (2020) proposed a simple age-sensitive SIR model that incorporates known age-interaction contact to examine the effect of age-heterogenous mitigations strategies for an infectious disease. They found out that for an epidemic like COVID-19, age-targeted mitigation strategies can significantly reduce mortalities and ICU use than homogeneous strategies. Modelling mitigation resulted in a 70% reduction in transmission rates in all populations except for a relaxed population.

Chen et al. (2020) proposed a time-dependent SIR model to track the transmission and recovery rate of COVID-19 at a discrete-time, t . To account for the impact of undetectable infections on the transmission of the disease, the authors considered two infection domains (detectable and undetectable infected persons) in the model. In this research, the author addressed the following questions; (1) When will the peak of the COVID-19 pandemic and when will it end if it could be contained, (2) If the disease cannot be contained, what is the proportion of the population needed to be infected to achieve herd immunity? (3) How

effective are the social distancing approaches to mitigate the spread of the disease? Using China as a case study, the authors obtained a one-day prediction error of about 3%.

Using China as a case study, Biswas et al. (2020) used the SIR model on a Euclidean network model to fit cumulative data into an empirical form. To justify that one requires a Euclidean model to fit the data, they calculated the number of cases recorded as a function of the Haversine distance, measured in Km, from the central point of COVID-19. Given some parameter values, the authors reported that the SIR model obtained a high accuracy on the data and predicted when the pandemic was expected to be over.

Improving the work of Chen et al. (2020) on developing a Bats-Hosts-Reservoir-People transmission network to simulate the transmission of SARS-CoV-2 from bats to humans, Gonzalez (2020) developed a SIR model based on the transmission of the disease from an individual to another. This model included some variables of containment measures taken worldwide. The authors modified the original model only to consider the vector and the host for populations where the disease was imported. By comparing different scenarios, the authors showed that the spread of the epidemic is strongly influenced by the measures of mitigation taken.

2.1.2 Susceptible-Exposed-Infected-Removed (SEIR)

Radulescu et al. (2020) studied the specific dynamics compartments and epidemic parameters of COVID-19 using a traditional SEIR model as it spreads in a population with people from all age groups. They examined the current control and mitigation strategy (social distancing, travel restrictions, and service interruptions) to generate predictions and analyze the efficiency of these control measures.

Guo et al. (2020) evaluated the transmission of COVID-19 with the basic reproductive number (R_0) using the SEIR model. They also examined the association between the transmission and propagation of the disease with temperature or humidity. The study outcomes presented a negative relationship between the high transmission of COVID-19 and temperature and humidity. They also presented a negative relationship between R_0 and humidity or temperature.

Zhan et al. (2020) integrated the SEIR model with daily intercity migration data to generate a model that explains the dynamics of COVID-19 in China. They collected the intercity travel data for 367 cities from Baidu Migration, a mobile application that records the movement of mobile phone users. They concluded that the infection rate of COVID-19 would reach its highest in most cities between mid-February to early March 2020.

Pandey et al. (2020) adopted the SEIR model and regression model with the John Hopkins University dataset on COVID-19 to analyse and predict the change in the transmission of the disease. They reported that the SEIR computed the R_0 as 2.02.

Prem et al. (2020) proposed an age-structured and location-specific SEIR model for several social distancing measures to analyse and predict the spread of COVID-19. The authors adapted this model under different scenarios of social distancing, travel restrictions, school closures, and workplace closure. They simulated the epidemic in Wuhan using this model over one year and found that control strategies aimed at reducing social contact could effectively reduce the spread of COVID-19.

Eikenberry et al. (2020) adapted the classical SEIR model to examine the impact of the public use of face masks on the dynamics and control of COVID-19. The author stratified the population into two strata depending on whether they used a mask in public. The model

assumes that some fraction of the population uses a face mask to protect themselves against the infection or prevent transmitting the disease. Under simulated epidemics and theoretical approaches, they found out that face masks, combined with other non-pharmaceutical control strategies, reduce the transmission of COVID-19 and should be employed worldwide.

Yang et al. (2021) developed a modified SEIR model that accounts for move-ins and move-outs in the susceptible and exposed population. Using the epidemic data in China, they predicted the timing of the peaks and size under different mitigation strategies.

Musa et al. (2021) proposed a deterministic model that incorporates several hospitalization measures for mild and severe COVID-19 cases to examine the effect of awareness programs on the transmission and propagation of COVID-19 in Nigeria. The authors stratified the susceptible population into compartments of susceptible aware individuals and susceptible unaware. The susceptible aware are well informed about the disease and follow all preventive measures, while the susceptible unaware do not follow the preventive measures set in place. They simulated the proposed model under three scenarios; (1) varying values to control parameters, (2) COVID-19 spreads faster in susceptible unaware population than in susceptible unaware population, and (3) simulation for contour plots for the basic reproductive number as a function of any two parameters chosen from the set of parameters in the model. They reported that parameters such as successful contact rate, modification parameter for decrease on infectiousness in an unaware susceptible population, COVID-19 induced death rates, the proportion of asymptomatic infected individuals, and severe hospitalization rates are essential to the model and should be prioritized in mitigating the transmission and propagation of the COVID-19 pandemic in Nigeria and around the world.

Khanjanchi et al. (2021) extended the SEIR model by incorporating contact tracing-hospitalizations strategies to study and predict the short- and long-term dynamics of COVID-

19. The model considered two groups of infected populations, the asymptomatic and symptomatic people, with the latter being a slower spreader of the disease. Based on the work by Gumel et al. (2004), the authors estimated the system parameters using the PRCC sensitivity analysis of 5 provinces of India and the Republic of India. They reported that social distancing drives the basic reproductive number lower, reducing the transmission rate of the SARS-CoV-2. They also concluded that the most effective control strategy is the isolation of all close contact

2.1.3 Other Models

Chen et al.(2020) proposed a Bats-Hosts-Reservoir-People (BHRP) transmission network model for modelling the transmission of SARS-CoV-2 from bats to humans. They also simplified the model to a Reservoir-People (RP) transmission model as it was difficult to examine the Bats-Hosts-Reservoir network, and the public was focused on the transmission from the reservoir to the people. They calculated the reproductive. The model divided the bats and hosts into susceptible, exposed, infected, and removed. They calculated the basic reproductive number, R_0 From the RP model using the next-generation matrix approach. The authors used the RP model to fit the data in Wuhan City, China, and found R_0 between two individuals to be 3.58. They also reported R_0 as 2.30 from the reservoir to person.

Crokidakis (2020) extended the SIR model by adding the Quarantined compartments to model the dynamics of COVID-19 in its early stages in Brazil. They reported that the number of confirmed cases and quarantined individuals grew exponentially. Vyasarayani and Chatterjee (2020) investigated the Susceptible-Exposed-Infectious-Quarantined-Recovered (SEIQR) model with time delays for latency and an asymptomatic phase. Their work simplified the work of Young et al. (2019) by ignoring the possibility of an individual losing their immunity to infections due to past diseases. As a result of this simplification, the model

decouples so that only the susceptible and infected populations are addressed. They then examined the effect of social distancing as a time-varying infection rate and found that a prolonged period of social distancing enforced early in the outbreak can lower the transmission rate without resulting in a loss of stability in the final state.

Wan et al. (2020) proposed a Markov Chain Monte Carlo (MCMC) model that incorporates COVID-19 control measures to evaluate the effect of partially lifting intervention measures on the dynamics of COVID-19 transmission. The authors grouped the populations into eight (8) compartments, namely susceptible (S), exposed (E), symptomatic (I), asymptomatic (A), isolated susceptible (S_i), quarantined infected pending confirmation (Q), hospitalized (H), and recovered (R). They considered recovered individuals to be immune during the pandemic. To better quantify the time-varying intervention measures, the authors assumed that the contact rate depends on the cumulative number of cases. Focusing on China, they reported the basic reproductive number with control measures, R_c for COVID-19 to be 3.36. They concluded that the current intervention and control measures must be kept if we are to reduce the spread of the infection.

Abioye et al. (2021) proposed a SEIQR model that incorporates three intervention measures, namely facemask with social distancing, prevention against reinfection, and treatment of the infected to minimize the transmission of COVID-19. They carried out a qualitative analysis of the model and showed that it has a globally asymptotically stable disease-free (Infection is zero) equilibrium if the basic reproductive number, $R_0 < 1$. Using this model to examine the dynamics of COVID-19 in Nigeria, they found out that the endemic could be significantly reduced or eradicated if the control measures are capable of driving R_0 below 1.

All of these researches have focused on modelling the COVID-19 pandemic to help understand the dynamics of the infection, detect the disease early and accurately, and

examine the effectiveness of current control strategies. However, they fail to incorporate vaccination into their model and to observe how vaccination changes the dynamics of COVID-19. Also, the authors failed to consider the interaction between information, vaccination, the spread of infection, and the perceived risk from the infection and vaccination. Furthermore, the authors did not consider how these factors change the population's behaviour toward the available control and mitigation strategies.

2.2 Vaccination And Game Theory

An individual's decision to vaccinate against infection is greatly influenced by the perceived risk of vaccination, the perceived risk of the infection, and their chance of being infected. The other people's decisions implicitly influence the individual's decision in the population, with the sum of these decisions giving the vaccine coverage, hence, the state of the infection in the population. Game theory predicts an individual's behaviour in scenarios where the payoff to the choice of an individual depends on the choices made by others in the population (Bauch and Earn, 2004).

Bauch and Earn (2004) incorporated a SIR model into a game theoretical framework to examine the population's behaviour, given that vaccine uptake is voluntary. They assumed that all individuals have access to the same information and use it in risk calculation. The authors considered an individual's strategy as his/her probability P of getting vaccinated and vaccine uptake level as the average of all strategies implemented by individuals in the population. The vaccine uptake level was assumed to be equal to the proportion of vaccinated individuals, p , in the population if there was no vaccine or disease-related death. They considered the payoff to a vaccinated individual and an unvaccinated individual as $-\tau_v$ and $-\tau_i\pi_p$ respectively, where τ_v , τ_i and π_p denote perceived risk from vaccination, perceived

risk from infection, and the probability that an unvaccinated person would eventually become infected. The expected payoff from vaccinating with probability P was expressed as;

$$E(P, p) = -rP - (1 - P)\pi_p \quad (2.1)$$

Where relative risk, $r = \frac{r_v}{r_i}$. Bauch and Earn (2004) reported that eradication threshold is greater than the expected vaccine uptake for any perceived relative risk. They reported that the threshold in perceived risk depends on the reproduction number R_0 .

3 MODEL FOR CO-EVOLUTION OF EPIDEMIC AND INFODEMIC

Over the years, several mathematical models have proven helpful in investigating and devising eradication plans for epidemic management. For example, a mathematical transmission model analysis was used to study the numerical spread of the 2014-2015 Ebola Virus Disease (EVD) and its eradication pathways. This helped investigators to make valuable suggestions to control the transmission of the disease (Jiang *et al.*, 2017). Similarly, for this work, the mathematical model employed is a stratified susceptible-infectious-susceptible (SIS) model for both the SARS-CoV-2 virus and information spread, which models the simultaneous progression of epidemic and infodemic. Therefore, this model has two domains: *disease and information domains*.

In the disease domain, the population is classified as either susceptible (S), infectious (I), or vaccinated (V). The population includes two mutually exclusive cohorts or strata in the information domain. These are:

- Individuals with good information who practice public behaviour-restrictive health measures aimed at reducing disease spread.
- Those with bad information contributing to the spread of the disease and bad information to others.

We model the spread of information as an infectious process, requiring some level of physical contact between the two sections of the information domain. Also, we assume that the fraction of the population "infected" with good information (I_G) follows the CDC safety guidelines and self-quarantine if they happen to get infected. Thus, only the fraction of the population that gets infected with bad information (I_B) contributes to the propagation and transmission of the disease and thus drives the spread of the epidemic. Hence, the importance

of spreading good information, instead of the bad, to mitigate the spread of the epidemic cannot be over-emphasized.

In this manuscript, we examine the roles of risk in vaccination, the weight of good information in risk calculation and the rates at which either good or bad information spreads, as these are key elements of the rather complex relationship between pandemic and infodemic. The model flow diagram is presented in Fig. 3.

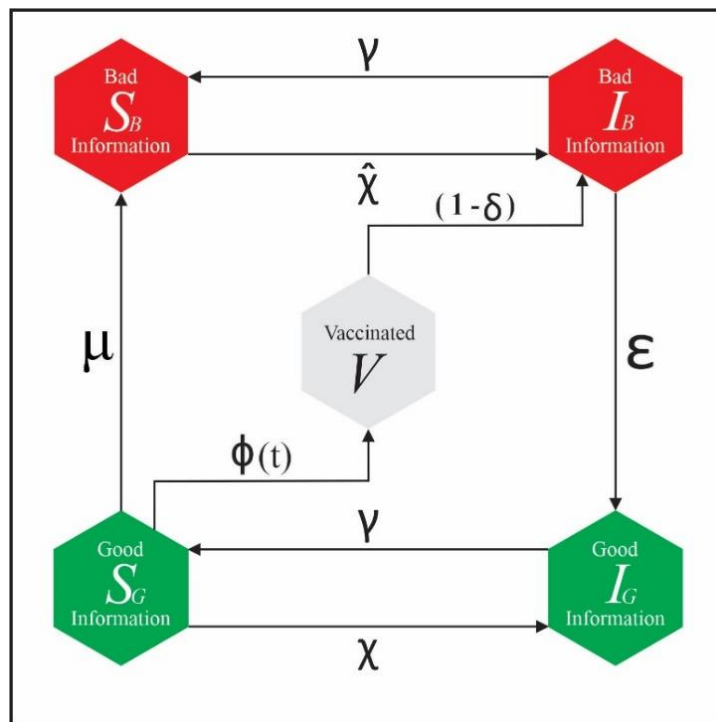


Figure 3.1 Schematic representation of the simultaneous progression of pandemic and infodemic with vaccination. Susceptible individuals with misinformation S_B have an increased force of infection $\hat{\chi} > \chi$. Susceptible individuals with good information S_G are infected with virus and misinformation at rates χ and μ respectively. Infected individuals with good information or bad information recover at the same rate γ . The misinformed infected I_B become educated at rate ϵ . Additionally, a susceptible person with good information S_G becomes vaccinated with probability ϕ . The leakage infection of the vaccinated population is asymptomatic and, therefore, unknowingly become I_B .

As seen in Figure 3.1, a susceptible person with good information, S_G can either be exposed to an infected person with bad behaviour, I_B to become infected with good behaviour, I_G or be exposed to bad information to become a susceptible individual with bad information, S_B at rate μ . When an infected person with bad behaviour, I_B recovers, he/she becomes susceptible with bad behaviour, S_B . The recovery rate is γ . Similarly, a bad-behaving infected person becomes educated at a rate of ϵ to become an infected person with good behaviour, I_G . This leads us to assume that the transmission rate of good information to an infected person with bad information is proportional or directly dependent upon their contact with those with good information. The susceptible person with good information S_G becomes vaccinated with probability ϕ . Those vaccinated are now considered temporarily immune to the disease, with efficacy of δ . The vaccination compartment serves as a vaccination leakage for $\delta < 1$.

In the absence of vital dynamics, we assume $S_G + S_B + I_G + I_B + V = 1$. We also assume that the two infected populations, I_B and I_G , both recovers at a rate γ . However, the susceptible persons with good behaviour, S_G are infected at a much lower rate than the susceptible with bad behaviour, S_B , such that $\chi < \hat{\chi}$.

We incorporate the theory of games with epidemic modelling to help understand population behaviour towards vaccination (Bauch and David, 2004). In this model, we assume that the probability of getting vaccinated depends on the weight of good information in risk calculation and relative risk (the risk perception of vaccination relative to infection), $r = \frac{r_v}{r_i}$, where r_i and r_v denotes risk perception of infection and vaccination, respectively. The probability ϕ that an individual chooses to vaccinate is determined by the strength of the initiative, m , and the reward when the vaccination strategy is implemented compared to when people do not vaccinate (Kabir and Tanimoto, 2020).

Based on the schematic representation (see Fig. 3.1) and assumptions above, we formulate a mathematical model for the co-evolution of pandemic and infodemic with vaccination given by the following six-dimensional ODE equations:

$$\frac{dS_G}{dt} = \gamma I_G - \phi S_G - \chi S_G I_B - \mu S_G (I_B + S_B) \quad (3.1)$$

$$\frac{dS_B}{dt} = \gamma I_B + \mu S_G (S_B + I_B) - \hat{\chi} S_B I_B \quad (3.2)$$

$$\frac{dI_G}{dt} = \epsilon (S_G + I_G) I_B - \gamma I_G + \chi S_G I_B \quad (3.3)$$

$$\frac{dI_B}{dt} = -\gamma I_B + \hat{\chi} S_B I_B - \epsilon (S_G + I_G) I_B + (1 - \delta) \chi V I_B \quad (3.4)$$

$$\frac{dV}{dt} = \phi S_G - (1 - \delta) \chi I_B V \quad (3.5)$$

$$\frac{d\phi}{dt} = m\phi(1 - \phi)(\alpha(S_G + I_G) + (I_B + I_G) - rV) \quad (3.6)$$

The wide use of various media outlets has made the spread of information faster than the spread of infection; however, the tendency for a person's decision or opinion about vaccination to change upon receiving information is highly unpredictable. Therefore, in our mean-field model, where information and physical networks are not separated, the information transmission rate (μ and ϵ) can be more or less than the rate of disease transmission. In our model, we assume that the rate of infection of bad-behaving individuals, $\hat{\chi}$, exceeds the spread of bad information, μ , ($\mu < \hat{\chi}$), and the rate at which an infected person with bad behaviour gets educated, ϵ , exceeds the inherent rate of recovery ($\epsilon > \gamma$).

Table 3.3.1 Interpretation of the state variables and parameters. All parameters are unitless, except for γ measured in 1/day

Variable	Description
S_G	Susceptible population with good information
I_G	Infected population with good information
S_B	Susceptible population with bad information
I_B	Infected population with bad information
V	Vaccinated population
ϕ	Probability of vaccination
Parameters	
μ	Misinformation: Rate of transmission of bad information to S_G
ε	Education: Rate of transmission of good information to I_B
γ	Recovery rate
r	Risk perception of vaccination relative to infection
δ	Vaccination efficacy
m	Strength of initiative or belief
χ	Probability of S_G becoming I_G through contact with I_B
$\hat{\chi}$	Probability of S_B becoming I_B through contact with I_B
α	Weight of good information in risk calculation

3.1 Game Theory and Vaccination: Deriving the Risk Function

In a vaccination game involving two kinds of players (the vaccinated, V , and the defector, U), provided with a finite set of choices π_V and π_U respectively, the payoff to a vaccinated individual will be more significant when the risk of vaccination (r_v) relative to infection (r_i) is smaller. We consider the defector (U) to take a chance of being infected (I). We consider the payoff of the vaccinated and infected interacting with each other and assumes that the payoff of the vaccinated/defector interacting with the vaccinated/defector is zero. We also assume that the individuals get exposed to some level of bad information and good information in terms of education, with the weight of good information with respect to the

epidemic size in the perceived risk for infection denoted as α . Since good information increases the risk perception of infection, the resulting payoff matrix is:

$$\pi = \begin{bmatrix} 0 & -r_v V \\ -r_i(\alpha G + I) & 0 \end{bmatrix} \quad (3.7)$$

Where $G = I_G + S_G$ and $I = I_B + I_G$. Since our game only considers two strategies, we denote the frequency of strategy selection of vaccination and refusing vaccination (infection) as ω_v and ω_i , such that $\omega_v + \omega_i = 1$. The replicator equations for each group of individuals follow:

$$\dot{\omega}_j = \omega_j [(\pi\omega)_j - \omega' \pi \omega] ; j = v, i \quad (3.8)$$

Since $\omega_v + \omega_i = 1$, the coupled replicator can be simplified to:

$$\dot{\omega} = \omega_v(1 - \omega_v)[(\pi\omega)_v - (\pi\omega)_i] \quad (3.9)$$

Where $(\pi\omega)_v - (\pi\omega)_i = \Delta E$ is the measure of the incentive for an individual to change strategies from infection to vaccination (Bauch and David, 2004; Hummert *et al.*, 2014). Since Eq.(3.7) models a coordination game where the most significant payoffs are along the main diagonal, we compute the pure Nash equilibrium by applying the Bishop-Cannings theorem that uses the relative difference in the diagonal elements (Hofbauer and Sigmund, 2003; Hummert *et al.*, 2014). Thus, the frequency of selection is:

$$\omega^* = \frac{\pi_{vi}}{\pi_{vi} + \pi_{iv}} \quad (3.10)$$

where π_{vi} and π_{iv} are the expected payoffs in Eq. (3.7). The marginal expected difference in the strategies is:

$$\Delta E = \omega^* E(v) - (1 - \omega^*) E(i) = -r_v V + r_i(\alpha G + I) \quad (3.11)$$

The game's dynamics will remain the same if the payoff function is scaled by a constant, eliminating one of the parameters. Hence, the marginal expected difference can be written as

$$\Delta E = \alpha G + I - \frac{r_v}{r_i} V = \alpha G + I - rV \quad (3.12)$$

Given Eq. (3.12), we can rewrite Eq.(3.9) as:

$$\dot{\omega} = \omega_v(1 - \omega_v)[\alpha G + I - rV] \quad (3.13)$$

If we substitute ω for ϕ , in Eq. (3.13) and multiply it by the strength of the initiative parameter, m simplifies the equation to Eq. (3.6).

3.2 Analytical Derivation of R_0 and R_e

The effective reproductive number, R_e , is a parameter used to measure the prevalence of infection and follow up a pandemic (Koo *et al.*, 2020). Unlike the basic reproductive number, R_0 that measures the expected number of new cases from an infected individual in a population where everyone is susceptible, R_e is the expected number of the newly infected individual by an infected individual at any given time. R_0 usually larger than R_e because R_e considers the effect of mitigation and control measures and the fraction of the population infected by or immune to the disease (Delamater *et al.*, 2019).

We derive the basic reproductive number using the concept of the next-generation matrix (Diekmann *et al.*, 1990; Driessche and Watmough, 2002). In the presence of vaccination, we solve for the non-trivial fixed point in equations (3.3 & 3.4) such that the probability of vaccination uptake $\phi \in (0,1)$. Eq. (3.3) leads to:

$$I_G = \frac{I_B (\epsilon G + \chi S_G)}{\gamma} ; \text{ where } I_B \neq 0 \text{ and } G = S_G + I_G \quad (3.14)$$

Then Eq. (3.4) becomes;

$$I_B \left(\frac{\hat{\chi} S_B + \chi(1-\delta)V}{\epsilon G + \gamma} - 1 \right) = 0 \quad (3.15)$$

Also, by adding Eq. (3.3 & 3.4) and substituting Eq. (3.14) into the result, we have;

$$I_B \left(\frac{\hat{\chi} S_B + \chi(1-\delta)V}{\gamma + \epsilon G} - 1 \right) = 0 \quad (3.16)$$

I_B converges to 0, and the system will reach a disease-free equilibrium (DFE) when the term in parenthesis in Eq. (3.16) is negative $\forall t \geq 0$. Hence, we have the effective reproductive number, R_e ;

$$R_e = \left(\frac{\hat{\chi}S_B + \chi(1-\delta)V}{\gamma + \epsilon G} - 1 \right) \quad (3.17)$$

When no vaccination is available, $\phi = 0 = V$, R_e becomes R_0 and becomes Eq. (3.18). Also, when $\delta = 1$, R_e becomes R_0 .

$$R_0 = \left(\frac{\hat{\chi}S_B}{\gamma + \epsilon G} - 1 \right) \quad (3.18)$$

The appearance of V in R_e is the evidence of vaccination leakage resulting in the vaccinated being re-infected. Observing R_e , we see that it decreases with increasing recovery rate, γ , and the spread of good information, ϵG . Increasing vaccine efficacy also decreases R_e and increasing the transmission rate of infection between the bad behaving people, $\hat{\chi}$.

3.3 Calculation of the Jacobian Matrix

Without loss of generality, we subject the system to restriction $S_G + S_B + I_G + I_B + V = 1$. Replacing I_G by $1 - S_G + S_B + I_B + V$ gives rise to linear dependency and a reduced model without Eq. (3.3). Given the state variable vector, $\vec{X} = [S_G, S_B, I_B, V, \phi]$, we calculate the Jacobian matrix by taking the first partial derivate of Eq. (3.1, 3.2 and 3.3 - 3.5). The (i, j) th element of the Jacobian matrix is the partial derivative of the i th equation with respect to the j th state variable. The resulting Jacobian matrix, J , is of the form

$$J = \begin{pmatrix} a_{11} & \cdots & a_{15} \\ \vdots & \ddots & \vdots \\ a_{51} & \cdots & a_{55} \end{pmatrix} \quad (3.22)$$

Row 1:

$$a_{11} = \gamma - [\phi + (\chi + \mu)I_B + \mu S_B]; \quad a_{12} = -\gamma - S_G \mu; \quad a_{13} = -\gamma - (\chi + \mu)S_G$$

$$a_{14} = -\gamma; \quad a_{15} = -S_G$$

Row 2:

$$a_{21} = \mu(S_B + I_B); a_{22} = \mu S_G - I_B \hat{\chi}; a_{23} = \mu S_G - (\hat{\chi} S_B - \gamma); a_{24} = 0; a_{25} = 0$$

Row 3:

$$a_{31} = 0; a_{32} = (\hat{\chi} + \epsilon)I_B; a_{33} = \hat{\chi}(S_B + \chi(1 - \delta)V - \gamma - \epsilon(1 - S_B - V))$$

$$a_{34} = I_B[\epsilon + \chi(1 - \delta)]; a_{35} = 0$$

Row 4:

$$a_{41} = \phi; a_{42} = 0; a_{43} = -(1 - \delta)\chi V; a_{44} = -\chi(1 - \delta)I_B; a_{45} = S_G$$

Row 5:

$$a_{51} = -m\phi(1 - \phi); a_{52} = a_{51}(\alpha + 1); a_{53} = a_{51}\alpha; a_{54} = a_{51}(\alpha + r + 1);$$

$$a_{55} = m(1 - 2\phi)[\alpha(1 - S_B - I_B - V) + (1 - S_B - S_G - V) - rV]$$

Observing the 5th column of the J matrix, we see that a branching point bifurcation exists for $S_G = 0$ and $\phi = 1$, resulting in an identical zero eigenvalue. The state variable vectors are calculated using numerical integration. $S_G = 0$ and $\phi \in (0,1)$ corresponds to the co-existence of pandemic and infodemic.

3.4 Obtaining the Nullclines

Given the state variable vector, $\vec{X} = [SG, SB, IB, V, \phi]$, we use the reduced model without Eq. (3.3) to obtain the nullclines. The nullclines for distinct pairs of the state variables are obtained by setting Eq. (3.1, 3.2, 3.4 – 3.6) to zero.

Let $\vec{x} = [X_1, X_2]$ be a state variable vector, and N_{x_1}, N_{x_2} be the nullclines in X_1 and X_2 respectively such that we have;

$$\frac{dX_1}{dt} = h_1(x_1, x_2) \tag{3.23}$$

$$\frac{dx_2}{dt} = h_2(x_1, x_2) \quad (3.24)$$

\mathfrak{N}_{x_1} is obtained by setting $h_1(x_1, x_2)$ equal to zero and solving for x_2 . Also, \mathfrak{N}_{x_2} is obtained by setting $h_2(x_1, x_2)$ equal to zero and solving for x_1 . Using this approach, we obtain our model's nullclines for pairs of state variables.

The S_B vs S_G nullclines are:

$$N_{S_B} = \frac{I_B(\hat{\chi}S_B - \gamma)}{\mu(S_B + I_B)} \quad (3.25)$$

$$N_{S_G} = \frac{\gamma I_B - S_G(\phi + (\chi + \mu)I_B)}{\mu S_G} \quad (3.26)$$

Substituting $\phi S_G / I_B = (1 - \delta)\chi V$, the I_B vs S_B nullclines are:

$$N_{S_B} = \frac{\mu S_G S_B}{\hat{\chi}S_B - \gamma - \mu S_G} \quad (3.27)$$

$$N_{I_B} = \frac{\gamma + \epsilon(I_G + S_G) - \frac{\phi S_G}{I_B}}{\hat{\chi}} \quad (3.28)$$

The I_B vs I_G nullclines are:

$$N_{I_G} = \frac{\gamma I_G}{\epsilon(I_G + S_G + \chi S_G)} \quad (3.29)$$

$$N_{I_B} = \frac{I_B[\chi(1-\delta)V - \epsilon S_G] + \mu(S_B + I_B)S_G}{\epsilon I_B} \quad (3.30)$$

The V vs I_B nullclines are:

$$N_{S_B} = \frac{\phi S_G}{\chi(1-\delta)V} \quad (3.31)$$

$$N_{I_B} = \frac{\gamma + \epsilon(I_G + S_G) - \hat{\chi}S_B}{(1-\delta)\chi} \quad (3.32)$$

The state variable vectors, $\vec{X} = [SG, SB, IB, V, \phi]$ are steady-state values obtained through numerical integration.

3.5 Perturbation About Fixed Points

Given the state variable vector, $\vec{X} = [x_1, x_2, x_3, x_4, x_5]$ of steady-state values, we obtain a time series of perturbed steady-state vectors, $\Delta = [\vartheta_1, \vartheta_2, \vartheta_3, \vartheta_4, \vartheta_5]$ using the steps below:

1. Generate a random variable, $\vec{u} = [u_1, u_2, \dots, u_5]$, such that $u_i \sim U(0,1)$
2. Obtain $\vartheta_i = (1 + \epsilon_0 (\sigma_i * u_i)) * x_i$, where ϑ_i is the *ith* component of the perturbed steady-state vector Δ , σ_i takes a value of 1 or -1 depending on whether $u_i - 0.5$ is negative or positive. That is, $\sigma_i = \text{sign}(u_i - 0.5)$. $\epsilon_0 \in (0,0.1)$ is the weight of the noise.

4 RESULTS AND DISCUSSION

Choosing a set of baseline parameters and initial conditions (Table 4.1), we examined the simultaneous progression of infodemic and COVID-19 pandemic when vaccination is available. We choose the recovery rate, γ , of an infected individual to reflect the 14-day incubation period, such that $\gamma = 0.07$. In our simulations, we assume that the probability of S_B becoming I_B , denoted as $\hat{\chi}$ is greater than the spread of misinformation, μ . We also assume the weight of good information to be unity, that is, $\alpha = 1$ throughout the simulations for r, δ, μ , and ϵ .

Table 4.4.1 Model parameters, state variables, and their baseline values. $\chi, \gamma, \hat{\chi}$ and m are kept constant throughout the analysis. $\alpha \neq 1$ for section 4.6

Variable	Description	Value
S_G	Susceptible population with good information	0.30
S_B	Susceptible population with bad information	0.50
I_B	Infected population with bad information	0.01
V	Vaccinated population	0.00
ϕ	Probability of vaccination	0.50
Parameters		
μ	Misinformation: Rate of transmission of bad information on S_G	0.10
ϵ	Education: Rate of transmission of good information on S_B	0.40
γ	Recovery rate	0.07
r	Risk perception of vaccination relative to infection	0.20
δ	Vaccination efficacy	0.90
m	Strength of initiative or belief	1.00
χ	Probability of S_G becoming I_G through contact with I_B	0.04
$\hat{\chi}$	Probability of S_B becoming I_B through contact with I_B	0.37
α	Weight of good information in risk calculation	1.00

We examine how infodemic, education, and vaccine efficacy drive COVID-19 disease transmission. We also observed how risk perception of vaccination relative to infection promotes vaccine uptake.

4.1 RICH DYNAMICAL PATTERNS OF THE MODEL

We observe five distinct patterns of dynamics throughout our simulation. These patterns are:

- a. ***Disease-free state***: also known as an epidemic-free state, occurred at extremely low misinformation, $\mu \approx 7e - 07$ (Figure 4.1 **A-C**). In this state, independent of education or risk perception, all variables achieve a steady state where $I_B = 0$ and $R_e < 1$.
- b. ***Periodic Small Outbreak***: at values of $r \in (0.127, 0.158)$ and $\mu \in (0.1, 0.144)$, all variables maintain low amplitude periodic cycles of epidemic spread with $I_B \approx 0.06, V \approx 0.68, \phi \approx 0.01, S_G \approx 0.03$ and $S_B \approx 0.22$ (Figure 4.1 **D-E**).
- c. ***Co-existence***: at low values of r and misinformation, $\mu \in (0.1, 0.144)$, the system transitions into a stable focus of high vaccination with $S_G \approx 0$ and a constant high-level infection $I_B \approx 0.18$. In addition, the probability of vaccination ϕ , jumps to 1.0 after about 1400 days (≈ 3.8 years) (Figure 4.2 **A - C**).
- d. ***Periodic Large Outbreak***: at $\mu = 0.1$ and $r \approx 0.274$, the system transitions into a low-frequency oscillation of high vaccination and low infection. We see an increase in the amplitude of oscillation of the susceptible and infected populations during the slow decay of V and a decrease when the jump in V happens (Figure 4.2 **D-F**). This pattern can be explained by considering Eq. (3.6 & 3.12), where $\Delta E = aG + I - rV$ switches sign due to slight changes in G, I , and V .
- e. ***Mixed Mode Oscillation***: at $\mu = 0.1, r = 3.587$, and $\epsilon = 0.450$, we observe an unstable high-frequency oscillation in I_B, S_B and S_G and low-frequency big jumps in V and ϕ happening in 1600 days (~ 4.38 years). The increase in the amplitude of

oscillation of the susceptible and infected populations occurs during the slow decay of V and decreases when the jump in V happens (Figure 4.3 A-C). Figure 4.3 (A-C) indicates that increasing ϵ when the perceived risk of vaccination is high will reduce the amplitude of infection without causing a change in vaccine uptake. This result suggests that reducing the spread of misinformation about the vaccine is essential to increasing vaccine uptake.

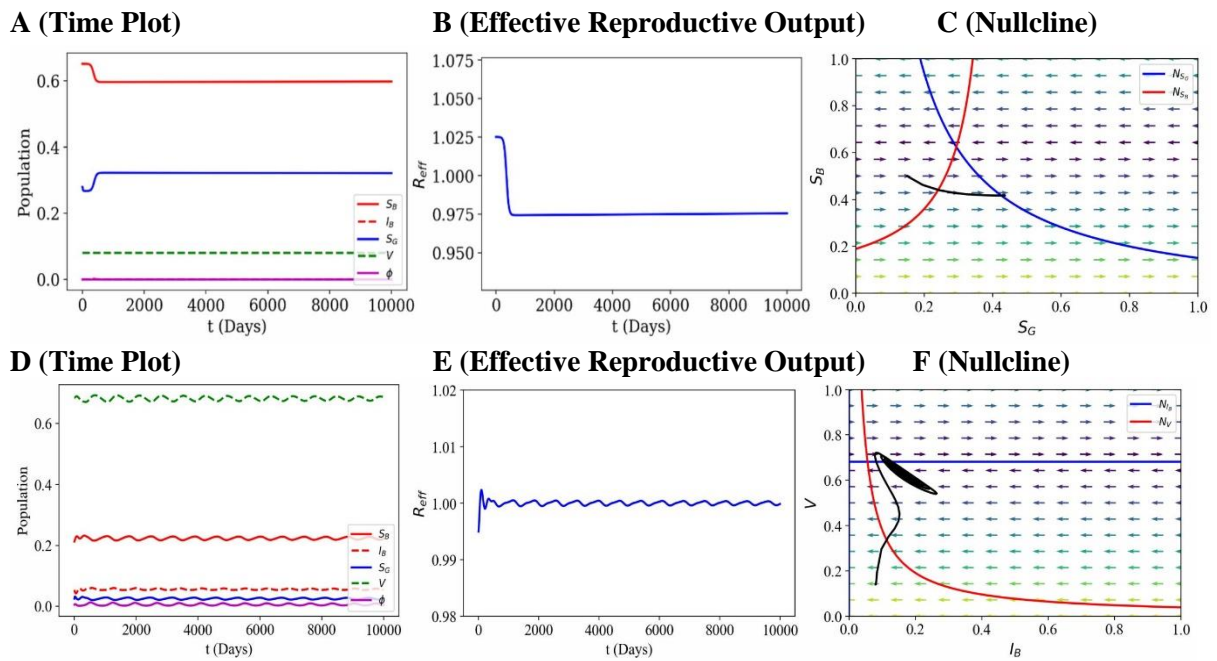


Figure 4.1 Simple dynamical patterns emerged from the model. **A - C**: Disease-free equilibrium (stable node). (At misinformation $\mu = 7e - 07$). **D - F**: Simple periodic oscillations (stable limit cycle). At risk $r \in (0.127, 0.158)$, misinformation $\mu \in (0.1, 0.144)$.

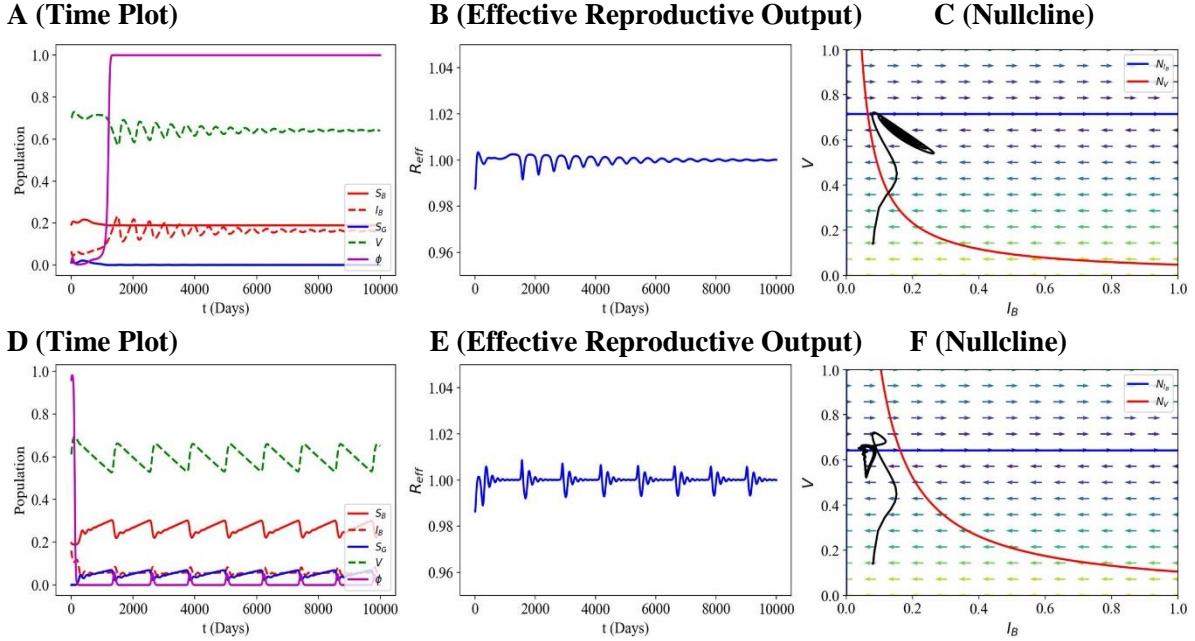


Figure 4.2 Simple dynamical pattern emerging from the model. A - C: Co-existence with high infection (stable focus). The other parameters are kept constant, as in Table 4.1. Initial conditions set about a perturbation of the steady states. D - F: Periodic large outbreaks at risk $r = 0.274$, misinformation $\mu = 0.1$. The other parameters are kept constant as in Table 4.1. Initial conditions set about a perturbation of the steady states.

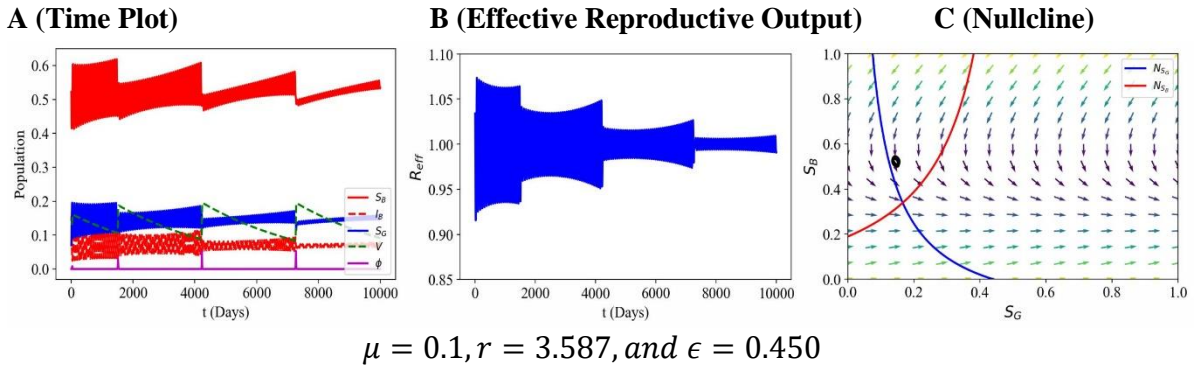


Figure 4.3 Complex dynamical pattern emerging from the model. A - C: Mixed Mode Oscillation at risk $r = 3.587$, misinformation $\mu = 0.1$, and education $\epsilon = 0.450$. The other parameters are kept constant as in Table 4.1. Initial conditions set about a perturbation of the steady states.

Comparing these results, we see that there are only three stable states in the system; $S_G = 0$, corresponding to co-existence with high vaccination, $I_B = 0$, corresponding to the disease-

free (DFE) equilibrium, and $\phi = 0$ corresponding to vaccine rejection. In addition, we observe that the spread of information plays an essential role in driving the pandemic.

4.2 LOW-RISK PERCEPTION OF VACCINATION PROMOTES VACCINE UPTAKE

Risk perception is vital in the decision to vaccinate and in vaccination behaviour (Schmid et al., 2017; Fan et al., 2021). To understand the role of risk perception in the acceptance of the COVID-19 vaccines and how it drives the pandemic, we consider the probability of vaccine uptake, ϕ to depend on the risk of vaccination relative to infection, r . The branching point bifurcation (BP) corresponding to the intersection of the limit cycle continuation (solid lines) and stable focus (dashed lines) separates the low-frequency stable oscillations of infection from the stable focus. In addition, the branching point corresponds to the point where $S_G = 0$ and $\phi = 1$ with an identical zero eigenvalue and $\Delta E = 0$ (Figure 4.4 **A - B**, Figure 4.5 **C - D**). The jumps in ϕ in Figure 4.5 (**C - D**) result from vaccine leakage, which is the 10% breakthrough infection; where vaccinated people get infected. Results indicate that increasing the risk perception of vaccination relative to infection increases infection and decreases vaccination, and vice-versa (Figure 4.4, Figure 4.5). These results concord with findings suggesting that a high-risk perception of infection promotes vaccine uptake (Caserotti et al., 2021, Patterson et al., 2022). High-risk perception of vaccination results in vaccine rejection, as seen by $\phi = 0$, driving the system to a stable focus of about 15% of the population getting vaccinated, with about 10% of the population getting infected. The system settles into endemic (equilibrium point) in about 2500 days (≈ 6.8 years) (Figure 4.4 **A - D**). At $r \approx 0.274$, the system transitions into a low-frequency stable oscillation of high vaccination ($\approx 65\%$) and about 10% infection. At lower values of risk ($r = 0.158$), the perceived risk of COVID-19 is higher when compared to vaccination; we observe that the system transitions into low amplitude stable oscillations of about 70% of the population getting vaccinated and

10% infected such that $\phi \in (0,1)$ (Figure 4.5 **A – B**). Decreasing the risk a little further to $r = 0.128$ drives the system into a stable focus of high vaccination with $S_G = 0$ and a constant high-level infection $I_B \approx 0.18$ with the probability of vaccination V , jumping to 1.0 after about 1400 days (Figure 4.5 **E – F**). From our results, we see that $S_G = 0$ corresponds to the co-existence of vaccination and epidemic. When $S_G = 0$, it is impossible to push vaccination further, as indicated in Figure 4.5 (**E – F**), where the entire population is not vaccinated but $\phi = 1$.

Notably, a high-risk perception of infection relative to vaccination increases vaccination and decreases infection. Therefore, to mitigate the spread of COVID-19, it is essential to promote educational messages emphasizing the risk associated with an infectious disease (in our case, COVID-19) and to increase the weight of good information about the safety and importance of the vaccination strategy available (Qiao et al., 2021).

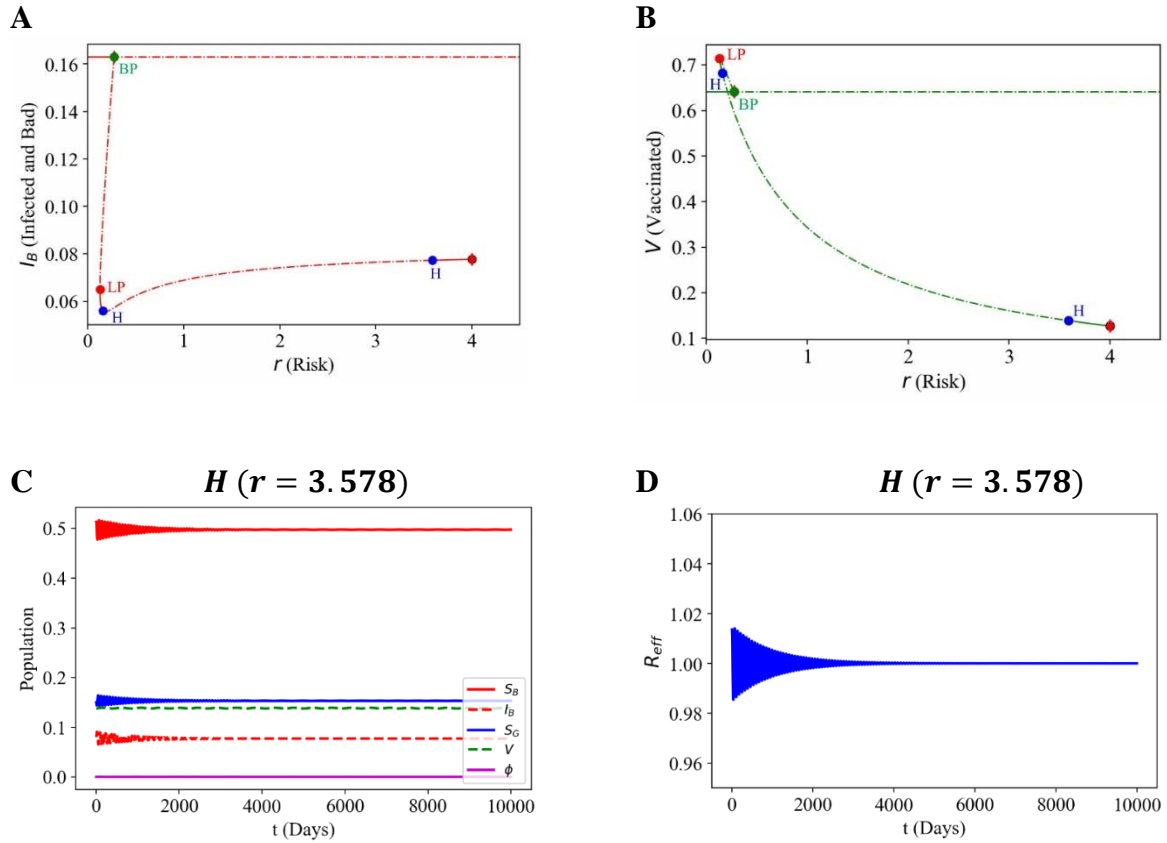


Figure 4.4: **A – B** Fixed Point with respect to risk r for infected with bad information and vaccination, respectively. The dashed and solid lines represent unstable and stable branches, respectively. The system undergoes a branching point bifurcation (BP) at $r = 0.274$, a saddle node bifurcation (LP) at $r = 0.128$ and two Hopf bifurcation (H) at $r = 3.587$ and $r = 0.158$. **C – D:** Time evolution of a perturbation of the H bifurcation at $r = 3.587$ corresponding to a stable focus and the effective reproductive number R_{eff} .

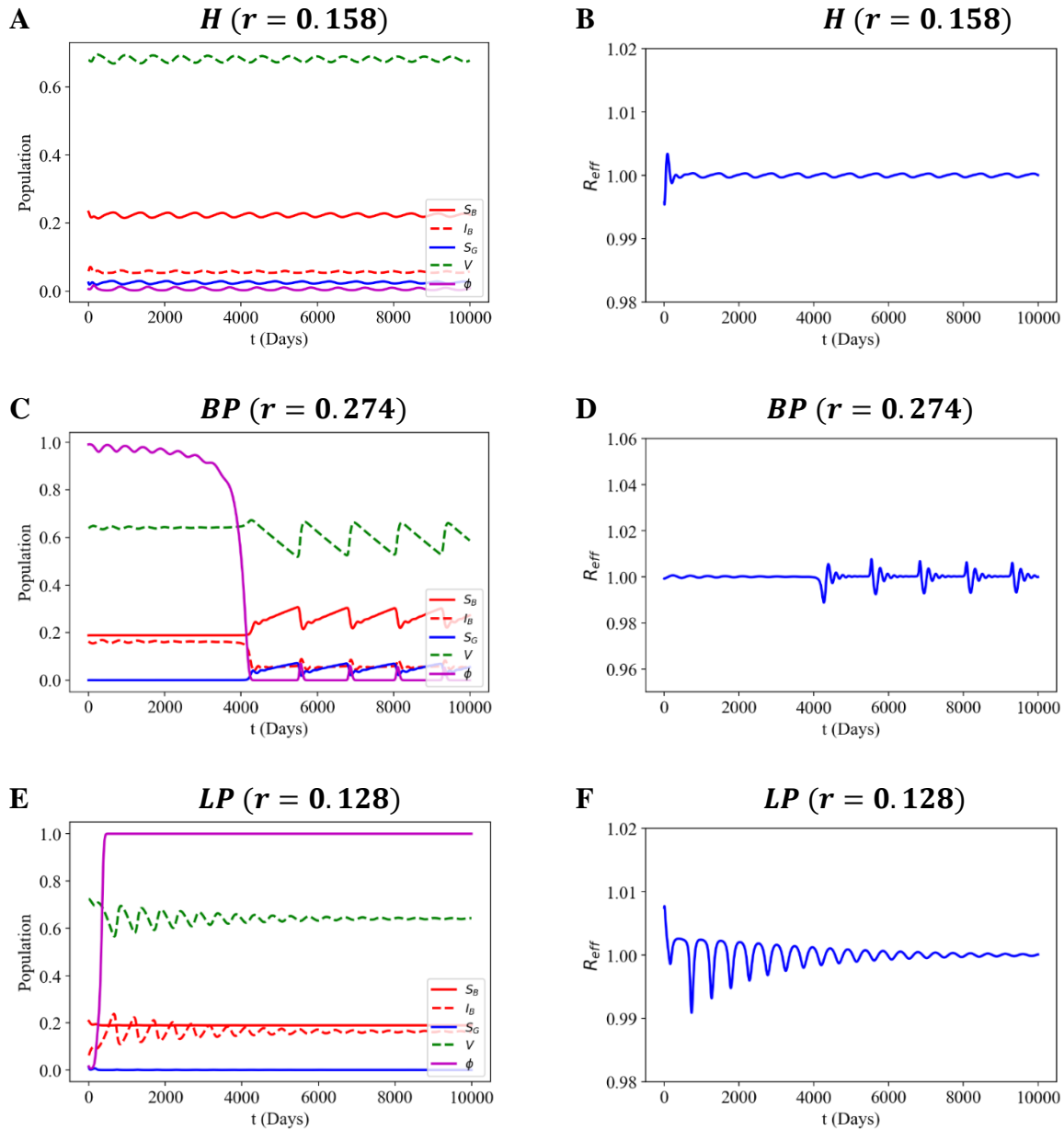


Figure 4.5 A – B: Time evolution of a perturbation of the H bifurcation with a pair of purely imaginary eigenvalue at $r = 0.158$ corresponding to a stable limit cycle of low amplitude and the effective reproductive number R_e . **C – D:** Time evolution of a perturbation of the BP bifurcation at $r = 0.274$ corresponding to a stable limit cycle and R_e . **E – F:** Time evolution of a perturbation of the saddle-node bifurcation LP at $r = 0.127$ corresponding to a stable focus of high amplitude & R_e

4.3 STOPPING MISINFORMATION IS NECESSARY TO STOP PANDEMIC

Misinformation is associated with increased health risk and vaccine hesitancy. Managing infodemic promotes the growth and maintenance of trust in the efficacy and safety of the vaccine, scientists, and healthcare (World Health Organization [WHO], 2021). To explain how the spread of misinformation promotes the spread of COVID-19, we examined how misinformation μ changes the system's behaviour when other parameters are constant. Results indicate increased risk and misinformation increase infection and lower vaccination. Conversely, a reduction in misinformation reduces infection and promotes vaccine uptake (Figure 4.6, Figure 4.7). We observe that increasing misinformation ($\mu = 0.144$) drives the system to a stable focus of high vaccination with $S_G = 0$ and a constant high-level infection $I_B \approx 0.18$ after about 1000 days (~ 2.7 years), corresponding to the co-existence of pandemic and infodemic (Figure 4.7 A – D). Without the management of misinformation, we have an epidemic; it is essential to stop misinformation to reach a disease-free state (Figure 4.7 E – F).

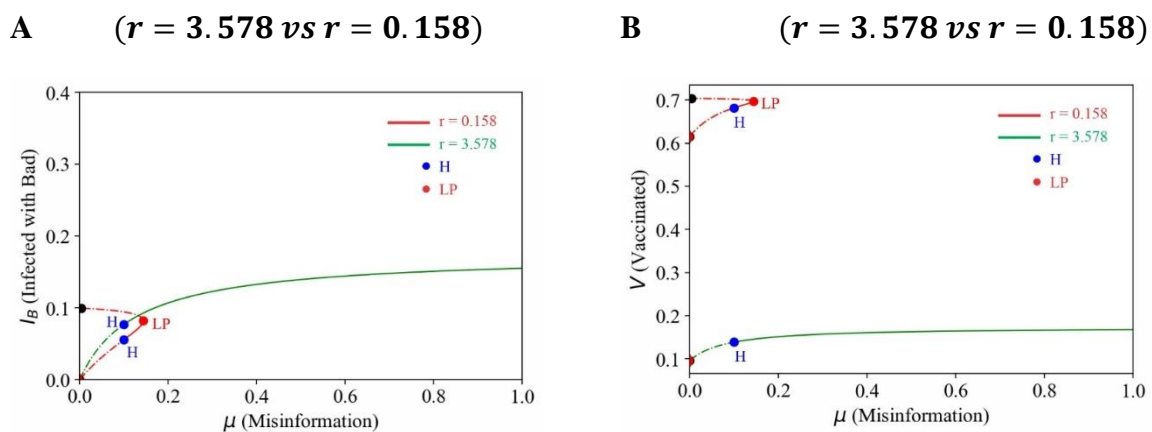


Figure 4.6: A – B: Fixed Point with respect to misinformation μ for Infected with bad information and vaccination, respectively for $r = 3.587$ vs $r = 0.158$. The dashed and solid lines represent unstable and stable branches, respectively.

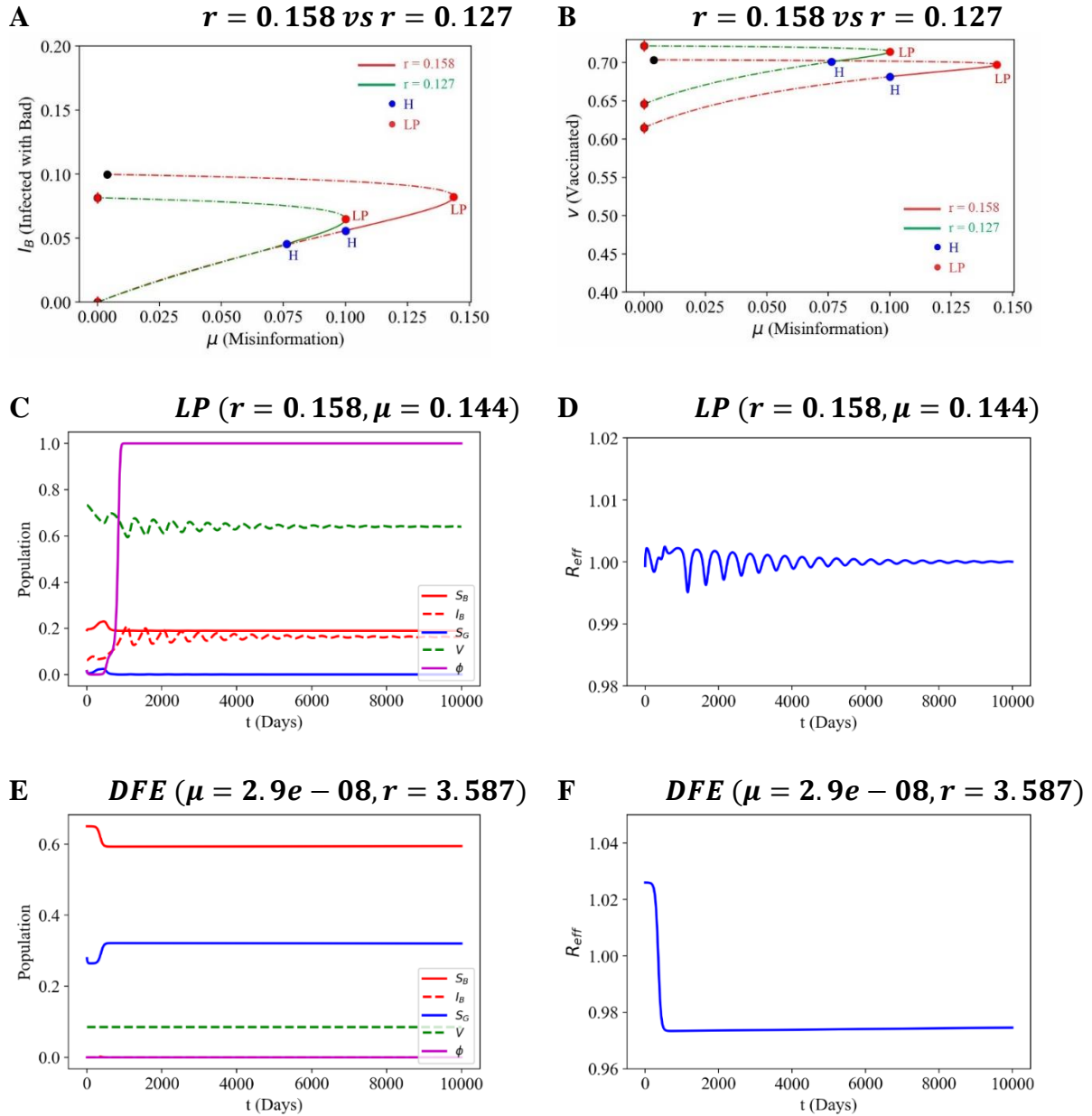


Figure 4.7: Fixed Point with respect to misinformation μ for Infected with bad information and vaccination, respectively for $r = 0.127$ vs $r = 0.158$. The dashed and solid lines represent unstable and stable branches, respectively. **C – D:** Time evolution of a perturbation of the saddle-node bifurcation LP at $\mu = 0.144$ corresponding to a stable focus of high vaccination and co-existence of infection & R_e . **E – F:** Disease-free equilibrium (stable node). (At misinformation $\mu = 2.9e - 08$)

4.4 INCREASING EDUCATION REDUCES INFECTION AND PROMOTES VACCINATION

Misinformation regarding COVID-19 has promoted unhealthy practices that have helped promote the incidence rate of the disease (Tasnim et al., 2020). Early provision of high-quality information, guidance, and promotion of its spread is needed to address misinformation. Also, approaches that improve the digital and health literacy of the population in recognizing facts from misinformation should be adopted (World Health Organization [WHO], 2021). To observe how promoting good information changes the population's behaviour toward vaccination, we examined how education, ϵ changes the system's dynamics when other parameters are constant. Promoting the spread of good information (education) drives the system to an unstable high-frequency oscillation of approximately 9% infection and a low-frequency oscillation of low vaccination (oscillating around 14%)(Figure 4.8 **E -F**). Our results indicate that even when the risk perception of vaccination relative to infection is high, increasing education decreases infection but does not cause a significant increase in vaccination (Figure 4.8 **A – B, E - F**). Conversely, decreasing education increases the infection's prevalence and lowers vaccination (Figure 4.8 **C – D**). Figure 4.8 (**C – D**) shows that inadequate promotion or lack of education (good information) amid misinformation drives the system to a steady state of high infection at 80%, zero vaccination with 20% of the population bad-behaving susceptible individuals. Also, Figure 4.8 (**C – D**) suggests that the entire population is misinformed or lacks accurate information about COVID-19 and its vaccination. These results suggest that mitigating the spread of bad information about the vaccine is necessary to reduce the perceived risk of vaccination relative to infection, resulting in a positive change in the population's behaviour towards vaccination. In addition, increasing the spread of good information at low-risk values increases vaccination and lowers infection (Figure 4.9 **A – B**). At intermediate values of education

($\epsilon = 0.337$), reducing the risk perception of vaccination ($r = 0.1578$) drives the system into a stable focus of about 65% vaccination with co-existence of infection ($\sim 20\%$) (Figure 4.9

A – D).

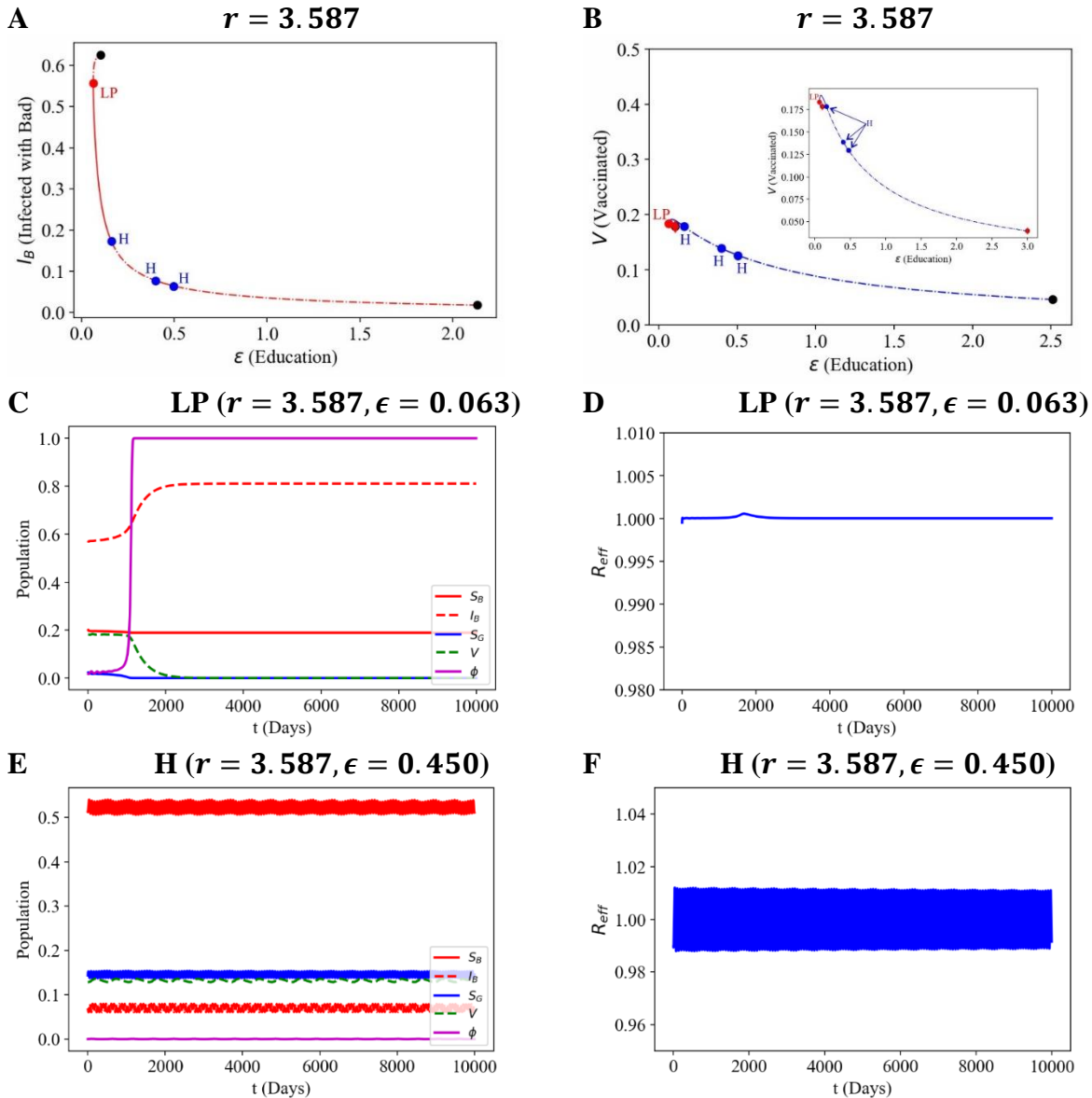


Figure 4.8: A – B: Fixed Point with respect to education ϵ for Infected with bad information and vaccination, respectively for $r = 3.587$. The dashed and solid lines represent unstable and stable branches, respectively. C – D: Time evolution of a perturbation of the LP bifurcation at $\epsilon = 0.063, r = 3.587$ corresponding to a steady state of zero vaccination, 80% infection and, 100% bad-behaving population & R_e . E – F: Time evolution of a perturbation of the H bifurcation at $\epsilon = 0.450, r = 3.587$ corresponding to stable oscillation of low infection & R_e .

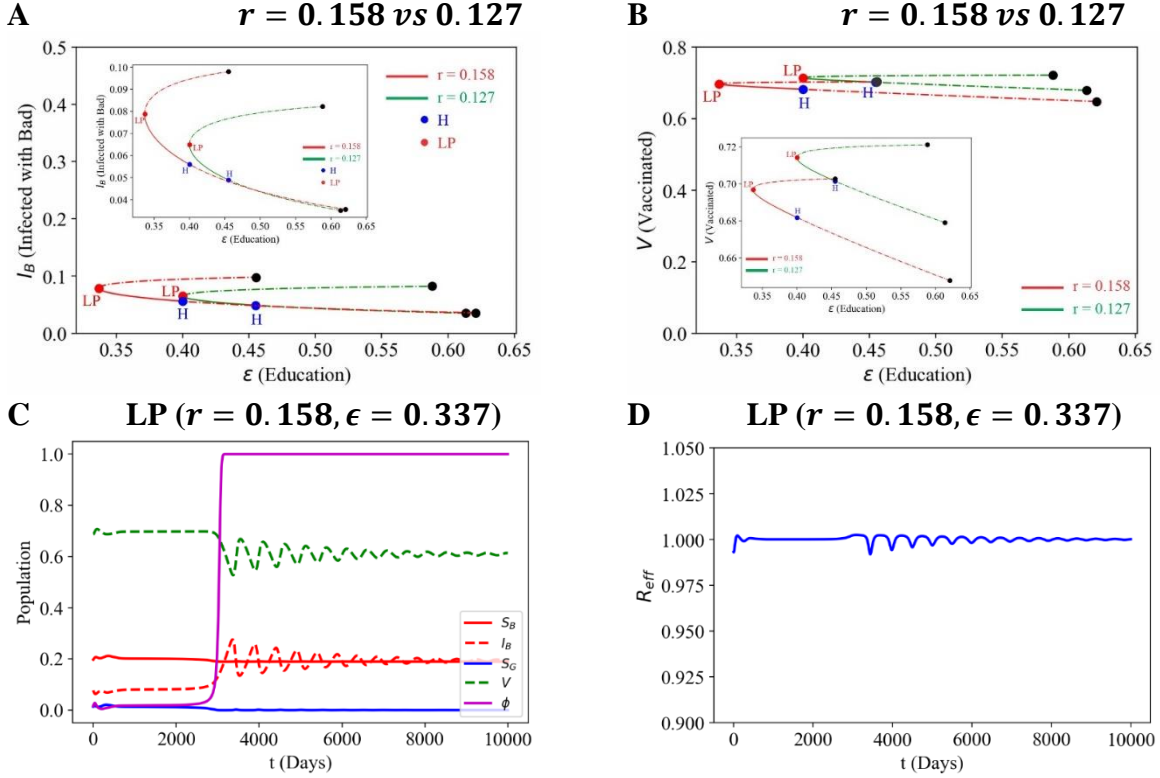


Figure 4.9: **A – B:** Fixed Point with respect to education ϵ for Infected with bad information and vaccination, respectively for $r = 0.158$ vs 0.127 . The dashed and solid lines represent unstable and stable branches, respectively. **C – D:** Time evolution of a perturbation of the LP bifurcation at $\epsilon = 0.337, r = 0.158$ corresponding to a stable focus of high vaccination and co-existence of infection & R_e .

4.5 HIGH VACCINE EFFICACY INHIBITS DISEASE TRANSMISSION

Vaccines reduce the susceptibility to infection, the number of infected individuals in a population, and death. Vaccine efficacy measures the extent to which a vaccine lowers the risk of getting infected (World Health Organization [WHO], 2021, September 18). High vaccine efficacy implies that vaccinated individuals are less likely to become infected than unprotected individuals. To evaluate the role of vaccine efficacy in reducing disease transmission when there is infodemic, we examine how protection δ drives the system. Our results indicate that when the perceived risk of vaccination is high, high vaccine efficacy reduces the severity of infectiousness but does not promote vaccine uptake (Figure 4.10, Figure 4.11). In Figure 4.11 (**A – D**), high vaccine efficacy drives the system to a stable

oscillation of about 7% and 13% of the population infected and vaccinated, respectively, with $\phi = 0$ indicating the rejection of the vaccine. At low-risk perception of vaccination, vaccine efficacy, δ at 0.826 drives the system to a stable focus of about 65% vaccination and 18% infection, which corresponds to the co-existence of vaccination and infection (Figure 4.10, Figure 4.12 A - B). Also, increasing the vaccine efficacy to 0.9 drives the system into low-frequency stable oscillation of high vaccination ($\sim 68\%$) and 6% infection (Figure 4.10, Figure 4.12 C - D). These results suggest that although high vaccine efficacy is necessary to impede the spread of infection, it is crucial to promote education and reduce the risk perception of vaccination for the population to accept the vaccine.

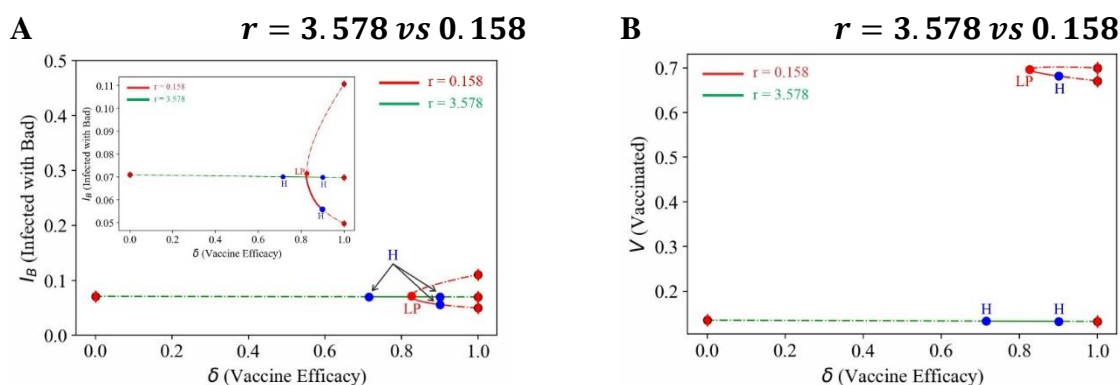


Figure 4.10 A – B: Fixed Point with respect to vaccine efficacy, δ for infected with bad information and vaccination, respectively for $r = 3.587$ vs $r = 0.158$. The dashed and solid lines represent unstable and stable branches, respectively.

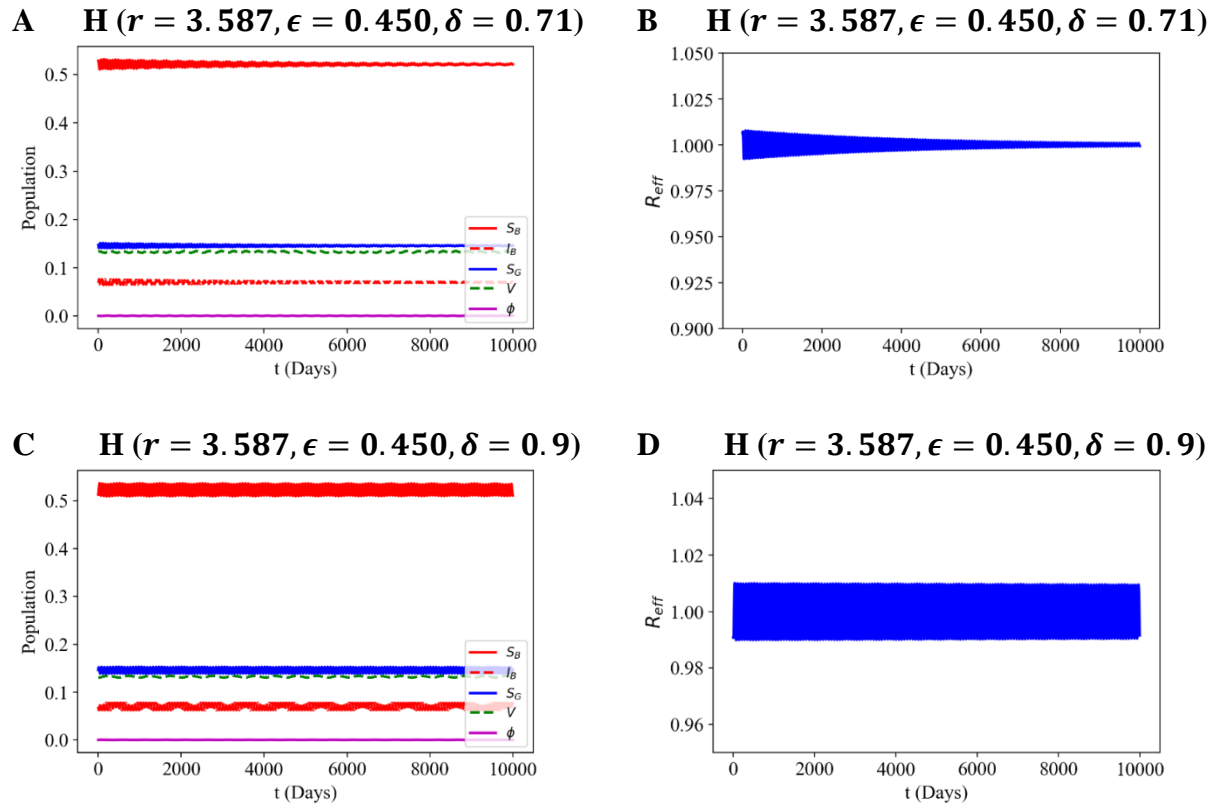


Figure 4.11: *A – B:* Time evolution of a perturbation of the H bifurcation at $r = 3.587, \epsilon = 0.450, \delta = 0.714$ corresponding to stable oscillation of 8% infection and low vaccination & R_e . *C – D:* Time evolution of a perturbation of the H bifurcation at $r = 3.587, \epsilon = 0.450, \delta = 0.900$ corresponding to stable oscillation of low vaccination & R_e .

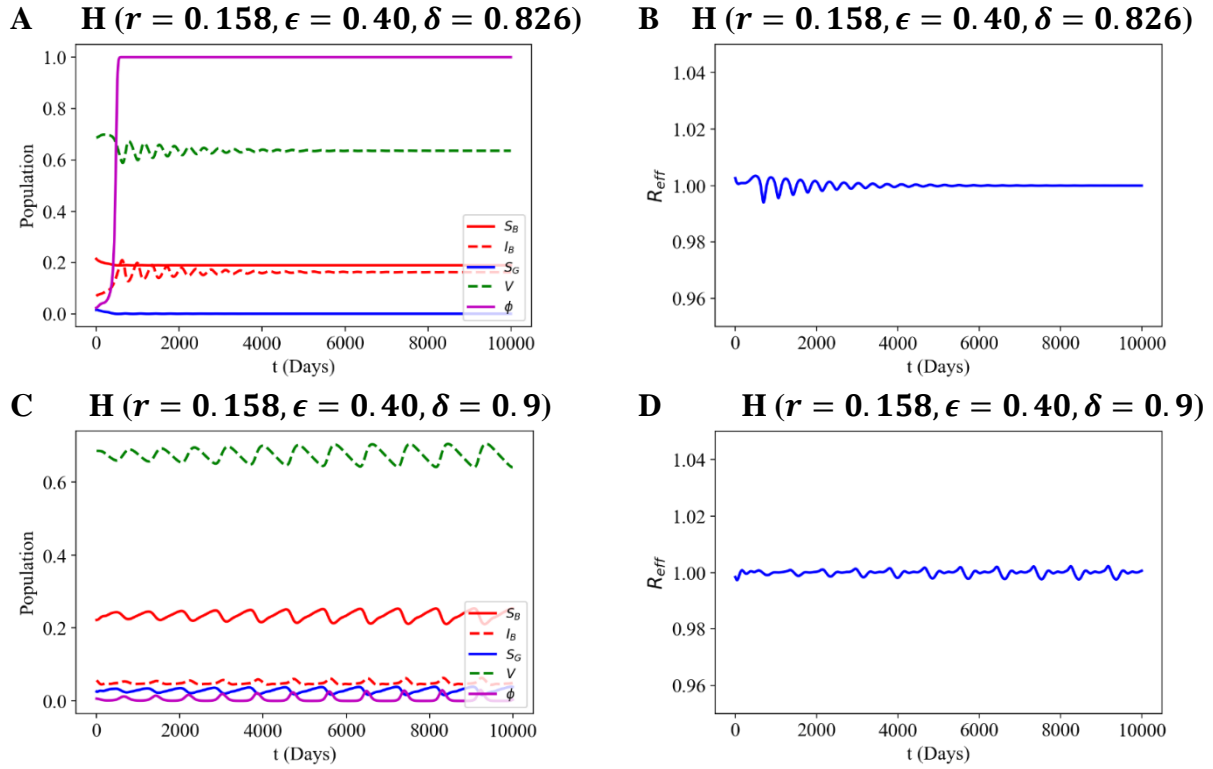


Figure 4.12: *A - D: Time evolution of a perturbation of the H bifurcation at $r = 0.158, \epsilon = 0.40, 1, \delta = 0.826$ drives the system to a stable focus of high vaccination and 18% infection corresponding to the co-existence of vaccination and infection & R_e . C - D: Time evolution of a perturbation of the H bifurcation at $r = 0.158, \epsilon = 0.40, 1, \delta = 0.900$ corresponding to stable oscillation of high vaccination & R_e .*

4.6 INCREASING THE WEIGHT OF GOOD INFORMATION PROMOTES VACCINATION AND DECREASES INFECTION

Promoting good information is crucial in stopping misinformation and impeding the spread of infection. To examine how the weight of good information influences the population's decision to vaccinate, we vary α and evaluate how it drives the system. Increasing the weight of good information drives down infection and increases vaccination (Figure 4.13). High-risk perception of vaccination and the weight of good information between zero and one, $\alpha \in [0,1)$ drives the system to a stable focus of low infection, $I_B \in [0.077,0.080)$. Also, increasing the weight of good information above unity ($\alpha \in [0,5]$) drives the system to an

unstable oscillation of lower infection such that, $I_B \in (0.077, 0.070)$ and increases vaccination (Figure 4.13 A-B, Figure 4.14 A). At low-risk perception of vaccination ($r = 0.158$) and weight of good information, $\alpha \approx 2.266$, the system transitions into a stable focus of about 65% vaccination and 18% infection with $S_G = 0$ corresponding to co-existence. Furthermore, it takes a higher weight of information, α , to arrive at a stable solution of lower infection and higher vaccination at lower risk, r (Figure 4.13 A – B, Figure 4.14 C). Comparing two values of misinformation given a low-risk perception of vaccination found that increasing the weight of good information shifts the stability such that lower misinformation results in higher vaccination and lower infection (Figure 4.14 D – E). Thus, a higher weight of good information does not change the system's dynamics much but shifts the stability.

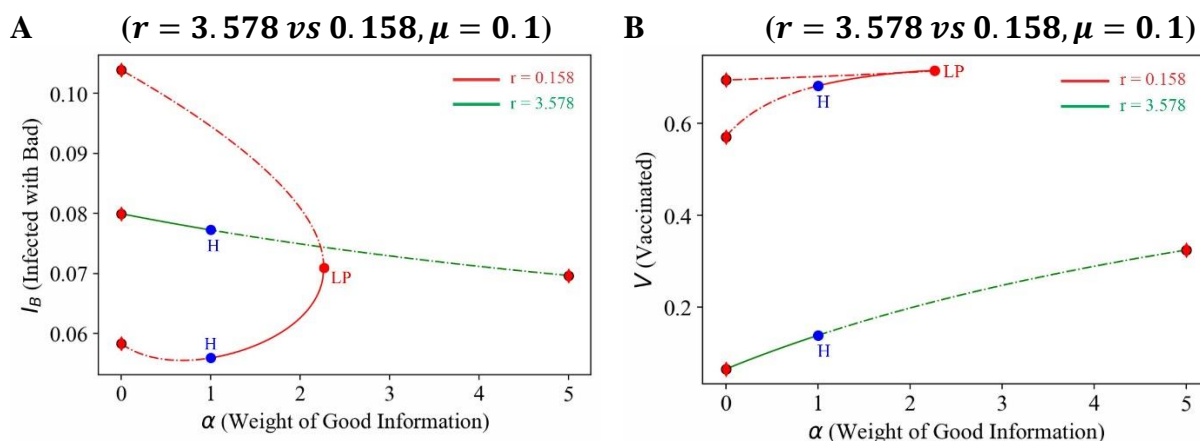


Figure 4.13: Fixed Point with respect to the weight of education, α for Infected with bad information and vaccination, respectively for $r = 3.587$ (green) vs $r = 0.158$ (red). The dashed and solid lines represent unstable and stable branches, respectively. Increasing the weight of good information increases vaccination.

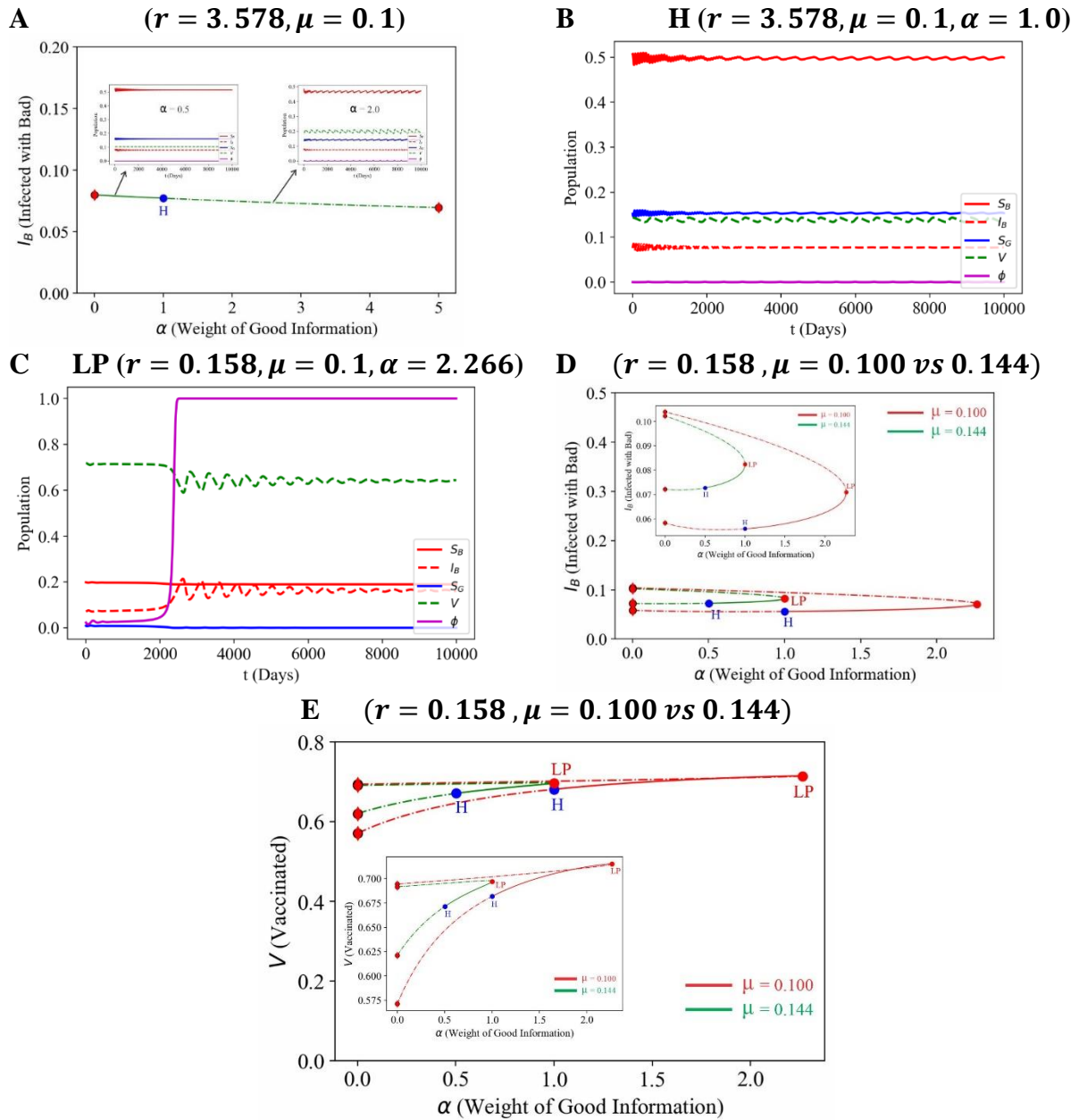


Figure 4.14: **A:** Fixed Point with respect to the weight of education, α for Infected with bad information for $r = 3.587$ and the time evolution in the stable (solid lines) and unstable region (dashed lines). **B:** Time evolution of a perturbation of the H bifurcation at $r = 3.587, \mu = 0.1, \alpha = 1.0$ with low vaccination. **C:** Time evolution of a perturbation of the L bifurcation at $r = 0.158, \mu = 0.1, \alpha = 2.266$ drives the system to a stable focus of high vaccination and 18% infection corresponding to the co-existence of vaccination and infection. **D – E:** Fixed Point with respect to the weight of education, α for Infected with bad information for $\mu = 0.1$ (red) vs 0.144 (green) when $r = 0.158$

5 CONCLUSION AND DISCUSSION

COVID-19 pandemic, a highly infectious disease caused by SARS - CoV -2 virus, has profoundly affected the world, leading to unprecedented health and socio-economic crisis. Non-pharmaceutical (NPIs) and pharmaceutical interventions (vaccination) have been adopted around the world to stop the spread of the COVID-19 pandemic. However, the success of vaccination largely depends on the decision of the population to get vaccinated and widespread belief about its benefits (Dror et al., 2020). COVID-19 and its vaccination have been accompanied by the overabundance of good information, misinformation, and disinformation, making it hard for the population to differentiate between facts and rumours. Misinformation regarding COVID-19 and its vaccination has promoted unhealthy practices among individuals that have helped propagate the spread of the infection. Another significant barrier to achieving herd immunity through vaccination is vaccine hesitancy, a strong reluctance or refusal to receive vaccination resulting from factors such as an individual's perceived risk of vaccination, distrust in scientists and healthcare providers, conspiracy theories, etc. (Lazarus et al., 2021; Rozek et al., 2021; Sallam et al., 2021).

To help understand the dynamics of COVID-19, we model the simultaneous progression of the COVID-19 pandemic and infodemic while accounting for the possibility of reinfection by the emerging new variants using an SIS compartmental model. We assume the information domain consists of correctly informed and misinformed individuals. We model the spread of information as an infectious process, requiring some level of physical contact between the two sections of the information domain. Also, we assume that the fraction of the population "infected" with good information follows the CDC safety guidelines and self-quarantine if they happen to get infected. Thus, only the fraction of the infected population with bad information contributes to the propagation and transmission of the infection. The population's

behaviour towards vaccination is observed by incorporating the theory of games into the SIS model under the assumption that vaccine uptake depends on the risk perception of vaccination relative to infection and contact with good information. In the system, three stable states were observed; $S_G = 0$, corresponding to co-existence with high vaccination (Figure 4.2 **A – C**), $I_B = 0$, corresponding to the disease-free (DFE) equilibrium (Figure 4.1 **A-C**), and $\phi = 0$ corresponding to vaccine rejection (Figure 4.4 **C - D**). We observe that a high-risk perception of vaccination drives the system to a stable focus of steady infection and vaccine rejection in about 6.8 years, corresponding to an endemic state (Figure 4.4 **A – D**). Conversely, a high-risk perception of infection relative to vaccination increases the vaccine. We see that the spread of misinformation plays a vital role in driving the pandemic. As propagation of infection is through those infected with misinformation, I_B , it is crucial to reduce the spread of misinformation if we are to stop the pandemic. At low misinformation, the epidemic ceases to spread regardless of the level of risk perception of vaccination (Figure 4.1 **A-C**, Figure 4.6, Figure 4.7). At high risk, reducing education in the presence of misinformation leads to an increased spread of infection and drives vaccination to zero (Figure 4.8 **C – D**). Education reduces the incidence rate of the infection for both low and high-risk perceptions of vaccination; however, a high-risk perception of vaccination does not increase the vaccinated population (Figure 4.8 **A – B, E – F**, Figure 4.9). In addition, increasing the weight of good information at high-risk perception of vaccination drives down the infection over a small range and increases vaccination (Figure 4.13, Figure 4.14 **A-C**). When the risk of vaccination is low, the weight of good information does not result in a significant change in the system's dynamics. Instead, it changes the system's stability with low risk requiring a higher weight of information to arrive at a stable solution of lower infection and higher vaccination (Figure 4.13, Figure 4.14). Notably, when vaccine efficacy is as high as 90%, reducing the spread of misinformation through the early dissemination and

promotion of good information is necessary to change the population's behaviour towards vaccination, achieve herd immunity and stop the pandemic.

In conclusion, stopping the COVID-19 infodemic is vital in preventing its spread and promoting vaccine uptake. As such, it is crucial to promote approaches that improve the digital and health literacy of the population in recognizing facts from misinformation (World Health Organization [WHO], 2021).

5.1 LIMITATIONS AND FUTURE DIRECTION

This research is limited in the assumption that every individual in the population is equally likely to become infected. In addition, our approach did not separate misinformation from disinformation, with the latter as a way to deceive people deliberately. Furthermore, modeling the spread of information as a compartmental model does not correctly account for the role of super spreaders on various social media platforms. As such, a social network may be incorporated into our model, with the information domain taking the form of a social network.

REFERENCES

- Abioye, A. I., Peter, O. J., Ogunseye, H. A., Oguntolu, F. A., Oshinubi, K., Ibrahim, A. A., & Khan, I. (2021). Mathematical model of COVID-19 in Nigeria with optimal control. *Results in Physics*, 28, 104598.
- Bae, S., Sung, E., & Kwon, O. (2021). Accounting for social media effects to improve the accuracy of infection models: combatting the COVID-19 pandemic and infodemic. *European Journal of Information Systems*, 30(3), 342-355.
- Betsch, C., Schmid, P., Heinemeier, D., Korn, L., Holtmann, C., & Böhm, R. (2018). Beyond confidence: Development of a measure assessing the 5C psychological antecedents of vaccination. *PloS one*, 13(12), e0208601.
- Biswas, K., Khaleque, A., & Sen, P. (2020). Covid-19 spread: Reproduction of data and prediction using a SIR model on Euclidean network. *arXiv preprint arXiv:2003.07063*.
- Caserotti, M., Girardi, P., Rubaltelli, E., Tasso, A., Lotto, L., & Gavaruzzi, T. (2021). Associations of COVID-19 risk perception with vaccine hesitancy over time for Italian residents. *Social science & medicine*, 272, 113688.
- Chen, T. M., Rui, J., Wang, Q. P., Zhao, Z. Y., Cui, J. A., & Yin, L. (2020). A mathematical model for simulating the phase-based transmissibility of a novel coronavirus. *Infectious diseases of poverty*, 9(1), 1-8.
- Chen, Y. C., Lu, P. E., Chang, C. S., & Liu, T. H. (2020). A time-dependent SIR model for COVID-19 with undetectable infected persons. *Ieee transactions on network science and engineering*, 7(4), 3279-3294.
- Chikina, M., & Pegden, W. (2020). Modeling strict age-targeted mitigation strategies for COVID-19. *PloS one*, 15(7), e0236237.

- Cinelli, M., Quattrocioni, W., Galeazzi, A., Valensise, C. M., Brugnoli, E., Schmidt, A. L., ... & Scala, A. (2020). The COVID-19 social media infodemic. *Scientific reports*, *10*(1), 1-10.
- Crokidakis, N. (2020). Modeling the early evolution of the COVID-19 in Brazil: Results from a Susceptible–Infectious–Quarantined–Recovered (SIQR) model. *International Journal of Modern Physics C*, *31*(10), 2050135.
- Datta, R., Yadav, A. K., Singh, A., Datta, K., & Bansal, A. (2020). The infodemics of COVID-19 amongst healthcare professionals in India. *Medical Journal Armed Forces India*, *76*(3), 276-283.
- Delamater, P. L., Street, E. J., Leslie, T. F., Yang, Y. T., & Jacobsen, K. H. (2019). Complexity of the basic reproduction number (R_0). *Emerging infectious diseases*, *25*(1), 1.
- Diekmann, O., Heesterbeek, J. A. P., & Metz, J. A. (1990). On the definition and the computation of the basic reproduction ratio R_0 in models for infectious diseases in heterogeneous populations. *Journal of mathematical biology*, *28*(4), 365-382.
- Dror, A. A., Eisenbach, N., Taiber, S., Morozov, N. G., Mizrachi, M., Zigran, A., ... & Sela, E. (2020). Vaccine hesitancy: the next challenge in the fight against COVID-19. *European journal of epidemiology*, *35*(8), 775-779.
- Eikenberry, S. E., Mancuso, M., Iboi, E., Phan, T., Eikenberry, K., Kuang, Y., ... & Gumel, A. B. (2020). To mask or not to mask: Modeling the potential for face mask use by the general public to curtail the COVID-19 pandemic. *Infectious disease modelling*, *5*, 293-308.
- Fan, C. W., Chen, I. H., Ko, N. Y., Yen, C. F., Lin, C. Y., Griffiths, M. D., & Pakpour, A. H. (2021). Extended theory of planned behavior in explaining the intention to COVID-19 vaccination uptake among mainland Chinese university students: an online survey study. *Human Vaccines & Immunotherapeutics*, *17*(10), 3413-3420.

- Glowacki, E. M., Lazard, A. J., Wilcox, G. B., Mackert, M., & Bernhardt, J. M. (2016). Identifying the public's concerns and the Centers for Disease Control and Prevention's reactions during a health crisis: An analysis of a Zika live Twitter chat. *American journal of infection control*, 44(12), 1709-1711.
- González, R. E. (2020). Different scenarios in the Dynamics of SARS-Cov-2 Infection: an adapted ODE model. *arXiv preprint arXiv:2004.01295*.
- Gumel, A. B., Ruan, S., Day, T., Watmough, J., Brauer, F., Van den Driessche, P., ... & Sahai, B. M. (2004). Modelling strategies for controlling SARS outbreaks. *Proceedings of the Royal Society of London. Series B: Biological Sciences*, 271(1554), 2223-2232.
- Guo, X. J., Zhang, H., & Zeng, Y. P. (2020). Transmissibility of COVID-19 in 11 major cities in China and its association with temperature and humidity in Beijing, Shanghai, Guangzhou, and Chengdu. *Infectious diseases of poverty*, 9(1), 1-13.
- Hajj Hussein, I., Chams, N., Chams, S., El Sayegh, S., Badran, R., Raad, M., ... & Jurjus, A. (2015). Vaccines through centuries: major cornerstones of global health. *Frontiers in public health*, 3, 269.
- Hofbauer, J., & Sigmund, K. (2003). Evolutionary game dynamics. *Bulletin of the American mathematical society*, 40(4), 479-519.
- Hummert, S., Bohl, K., Basanta, D., Deutsch, A., Werner, S., Theißen, G., ... & Schuster, S. (2014). Evolutionary game theory: cells as players. *Molecular BioSystems*, 10(12), 3044-3065
- Jiang, S., Wang, K., Li, C. et al. Mathematical models for devising the optimal Ebola virus disease eradication. *J Transl Med* 15, 124 (2017). <https://doi.org/10.1186/s12967-017-1224-6>

- Kabir, K. A., & Tanimoto, J. (2020). Evolutionary game theory modelling to represent the behavioural dynamics of economic shutdowns and shield immunity in the COVID-19 pandemic. *Royal Society open science*, 7(9), 201095.
- Khajanchi, S., Sarkar, K., Mondal, J., Nisar, K. S., & Abdelwahab, S. F. (2021). Mathematical modeling of the COVID-19 pandemic with intervention strategies. *Results in Physics*, 25, 104285.
- Khan, Y. H., Mallhi, T. H., Alotaibi, N. H., Alzarea, A. I., Alanazi, A. S., Tanveer, N., & Hashmi, F. K. (2020). Threat of COVID-19 vaccine hesitancy in Pakistan: the need for measures to neutralize misleading narratives. *The American journal of tropical medicine and hygiene*, 103(2), 603.
- Khoshnaw, S. H., Salih, R. H., & Sulaimany, S. (2020). Mathematical modelling for coronavirus disease (COVID-19) in predicting future behaviours and sensitivity analysis. *Mathematical Modelling of Natural Phenomena*, 15, 33.
- Koo, J. R., Cook, A. R., Park, M., Sun, Y., Sun, H., Lim, J. T., ... & Dickens, B. L. (2020). Interventions to mitigate early spread of SARS-CoV-2 in Singapore: a modelling study. *The Lancet Infectious Diseases*, 20(6), 678-688.
- Kreps, S. E., & Kriner, D. L. (2020). Model uncertainty, political contestation, and public trust in science: Evidence from the COVID-19 pandemic. *Science advances*, 6(43), eabd4563.
- Lazarus, J. V., Ratzan, S. C., Palayew, A., Gostin, L. O., Larson, H. J., Rabin, K., ... & El-Mohandes, A. (2021). A global survey of potential acceptance of a COVID-19 vaccine. *Nature medicine*, 27(2), 225-228
- MacDonald, N. E. (2015). Vaccine hesitancy: Definition, scope and determinants. *Vaccine*, 33(34), 4161-4164.

- Marzo, R. R., Sami, W., Alam, M., Acharya, S., Jermsittiparsert, K., Songwathana, K., ... & Yi, S. (2022). Hesitancy in COVID-19 vaccine uptake and its associated factors among the general adult population: a cross-sectional study in six Southeast Asian countries. *Tropical Medicine and Health*, 50(1), 1-10.
- Mills, M., Rahal, C., Brazel, D., Yan, J., & Gieysztor, S. (2020). COVID-19 vaccine deployment: Behaviour, ethics, misinformation and policy strategies. *London: The Royal Society & The British Academy*.
- Mohamadou, Y., Halidou, A., & Kapen, P. T. (2020). A review of mathematical modeling, artificial intelligence and datasets used in the study, prediction and management of COVID-19. *Applied Intelligence*, 50(11), 3913-3925.
- Murayama, T., Wakamiya, S., Aramaki, E., & Kobayashi, R. (2021). Modeling the spread of fake news on Twitter. *Plos one*, 16(4), e0250419.
- Musa, S. S., Qureshi, S., Zhao, S., Yusuf, A., Mustapha, U. T., & He, D. (2021). Mathematical modeling of COVID-19 epidemic with effect of awareness programs. *Infectious disease modelling*, 6, 448-460.
- Naeem, S. B., Bhatti, R., & Khan, A. (2021). An exploration of how fake news is taking over social media and putting public health at risk. *Health Information & Libraries Journal*, 38(2), 143-149.
- Neumann-Böhme, S., Varghese, N. E., Sabat, I., Barros, P. P., Brouwer, W., van Exel, J., ... & Stargardt, T. (2020). Once we have it, will we use it? A European survey on willingness to be vaccinated against COVID-19. *The European Journal of Health Economics*, 21(7), 977-982.
- Nicola, M., Alsafi, Z., Sohrabi, C., Kerwan, A., Al-Jabir, A., Iosifidis, C., ... & Agha, R. (2020). The socio-economic implications of the coronavirus pandemic (COVID-19): A review. *International journal of surgery*, 78, 185-193.

- Nusair, M. B., Arabyat, R., Khasawneh, R., Al-Azzam, S., Nusir, A. T., & Alhayek, M. Y. (2022). Assessment of the relationship between COVID-19 risk perception and vaccine acceptance: a cross-sectional study in Jordan. *Human Vaccines & Immunotherapeutics*, *18*(1), 2017734.
- Pandey, G., Chaudhary, P., Gupta, R., & Pal, S. (2020). SEIR and Regression Model based COVID-19 outbreak predictions in India. *arXiv preprint arXiv:2004.00958*.
- Patterson, N. J., Paz-Soldan, V. A., Oberhelman, R., Moses, L., Madkour, A., & Miles, T. T. (2022). Exploring perceived risk for COVID-19 and its role in protective behavior and COVID-19 vaccine hesitancy: a qualitative study after the first wave. *BMC Public Health*, *22*(1), 1-11.
- Prem, K., Liu, Y., Russell, T. W., Kucharski, A. J., Eggo, R. M., Davies, N., ... & Klepac, P. (2020). The effect of control strategies to reduce social mixing on outcomes of the COVID-19 epidemic in Wuhan, China: a modelling study. *The Lancet Public Health*, *5*(5), e261-e270.
- Puri, N., Coomes, E. A., Haghbayan, H., & Gunaratne, K. (2020). Social media and vaccine hesitancy: new updates for the era of COVID-19 and globalized infectious diseases. *Human vaccines & immunotherapeutics*, *16*(11), 2586-2593.
- Qiao, S., Tam, C. C., & Li, X. (2021). Risk exposures, risk perceptions, negative attitudes toward general vaccination, and COVID-19 vaccine acceptance among college students in South Carolina. *American Journal of Health Promotion*, 08901171211028407.
- Rădulescu, A., Williams, C., & Cavanagh, K. (2020). Management strategies in a SEIR-type model of COVID 19 community spread. *Scientific reports*, *10*(1), 1-16.
- Rhodes, A., Hoq, M., Measey, M. A., & Danchin, M. (2021). Intention to vaccinate against COVID-19 in Australia. *The Lancet Infectious Diseases*, *21*(5), e110.

- Rozek, L. S., Jones, P., Menon, A., Hicken, A., Apsley, S., & King, E. J. (2021). Understanding vaccine hesitancy in the context of COVID-19: the role of trust and confidence in a seventeen-country survey. *International journal of public health*, 66
- Sallam, M., Dababseh, D., Eid, H., Al-Mahzoum, K., Al-Haidar, A., Taim, D., ... & Mahafzah, A. (2021). High rates of COVID-19 vaccine hesitancy and its association with conspiracy beliefs: a study in Jordan and Kuwait among other Arab countries. *Vaccines*, 9(1), 42.
- Shen, Z. H., Chu, Y. M., Khan, M. A., Muhammad, S., Al-Hartomy, O. A., & Higazy, M. (2021). Mathematical modeling and optimal control of the COVID-19 dynamics. *Results in Physics*, 31, 105028.
- Singh, R., & Adhikari, R. (2020). Age-structured impact of social distancing on the COVID-19 epidemic in India. *arXiv preprint arXiv:2003.12055*.
- Soares, P., Rocha, J. V., Moniz, M., Gama, A., Laires, P. A., Pedro, A. R., ... & Nunes, C. (2021). Factors associated with COVID-19 vaccine hesitancy. *Vaccines*, 9(3), 300.
- Tasnim, S., Hossain, M. M., & Mazumder, H. (2020). Impact of rumors and misinformation on COVID-19 in social media. *Journal of preventive medicine and public health*, 53(3), 171-174.
- The Lancet Infectious Diseases Editorial Board. The COVID-19 infodemic. *Lancet Infect Dis*. 2020;20:875.
- Tran, T., & Lee, K. (2016, August). Understanding citizen reactions and Ebola-related information propagation on social media. In *2016 IEEE/ACM International Conference on Advances in Social Networks Analysis and Mining (ASONAM)* (pp. 106-111). IEEE.
- Van den Driessche, P., & Watmough, J. (2002). Reproduction numbers and sub-threshold endemic equilibria for compartmental models of disease transmission. *Mathematical biosciences*, 180(1-2), 29-48.

- Vicente, N. E., & Cordero Jr, D. A. (2021). In the service of the Filipino: the role of Catholic higher education institutions in promoting COVID-19 vaccines in the Philippines. *Journal of Public Health, 43*(2), e377-e378.
- Vyasarayani, C. P., & Chatterjee, A. (2020). New approximations, and policy implications, from a delayed dynamic model of a fast pandemic. *Physica D: Nonlinear Phenomena, 414*, 132701.
- Wan, H., Cui, J. A., & Yang, G. J. (2020). Risk estimation and prediction by modeling the transmission of the novel coronavirus (COVID-19) in mainland China excluding Hubei province. *medRxiv*.
- Wang, L., Zhou, Y., He, J., Zhu, B., Wang, F., Tang, L., ... & Song, P. X. (2020). An epidemiological forecast model and software assessing interventions on the COVID-19 epidemic in China. *Journal of Data Science, 18*(3), 409-432.
- World Health Organization (WHO). Ten Threats to Global Health in 2019. 2019. Available online: <https://www.who.int/newsroom/spotlight/ten-threats-to-global-health-in-2019> (accessed on December 20 2020)
- World Health Organization. (2021). Infodemic management: an overview of infodemic management during COVID-19, January 2020–May 2021.
- World Health Organization. (2021). Vaccine efficacy, effectiveness and protection. *Retrieved September, 18, 2021*.
- Yang, K. C., Pierri, F., Hui, P. M., Axelrod, D., Torres-Lugo, C., Bryden, J., & Menczer, F. (2021). The covid-19 infodemic: Twitter versus facebook. *Big Data & Society, 8*(1), 205395172111013861.

- Yang, Z., Zeng, Z., Wang, K., Wong, S. S., Liang, W., Zanin, M., ... & He, J. (2020). Modified SEIR and AI prediction of the epidemics trend of COVID-19 in China under public health interventions. *Journal of thoracic disease*, *12*(3), 165.
- Young, L. S., Ruschel, S., Yanchuk, S., & Pereira, T. (2019). Consequences of delays and imperfect implementation of isolation in epidemic control. *Scientific reports*, *9*(1), 1-9.
- Zhan, C., Tse, C. K., Fu, Y., Lai, Z., & Zhang, H. (2020). Modeling and prediction of the 2019 coronavirus disease spreading in China incorporating human migration data. *Plos one*, *15*(10), e0241171.
- Zhang, S., Pian, W., Ma, F., Ni, Z., & Liu, Y. (2021). Characterizing the COVID-19 infodemic on Chinese social media: Exploratory study. *JMIR public health and surveillance*, *7*(2), e26090.
- Zhang, S., Pian, W., Ma, F., Ni, Z., & Liu, Y. (2021). Characterizing the COVID-19 infodemic on Chinese social media: Exploratory study. *JMIR public health and surveillance*, *7*(2), e26090.
- Zhao, Z. Y., Zhu, Y. Z., Xu, J. W., Hu, Q. Q., Lei, Z., Rui, J., ... & Chen, T. M. (2020). A mathematical model for estimating the age-specific transmissibility of a novel coronavirus. *Medrxiv*.